Published online 24 February 2016 *Nucleic Acids Research, 2016, Vol. 44, No. 8* ***3845–3864***
doi: 10.1093/nar/gkw099

The oncogenic triangle of HMGA2, LIN28B and IGF2BP1 antagonizes tumor-suppressive actions of the let-7 family

Bianca Busch[1,†], Nadine Bley[1,†], Simon Müller[1,†], Markus Glaß[1], Danny Misiak[1], Marcell Lederer[1], Martina Vetter[2], Hans-Georg Strauß[2], Christoph Thomssen[2] and Stefan Hüttelmaier[1,*]

[1]Institute of Molecular Medicine, Section for Molecular Cell Biology, Faculty of Medicine, Martin-Luther-University Halle Wittenberg, ZAMED, Heinrich-Damerow-Str.1, 06120 Halle, Germany and [2]Clinic of Gynecology, Faculty of Medicine, Martin-Luther-University Halle Wittenberg, Ernst-Grube-Straße 40, 06120 Halle, Germany

Received September 06, 2015; Revised January 13, 2016; Accepted February 11, 2016

ABSTRACT

The tumor-suppressive let-7 microRNA family targets various oncogene-encoding mRNAs. We identify the let-7 targets HMGA2, LIN28B and IGF2BP1 to form a let-7 antagonizing self-promoting oncogenic triangle. Surprisingly, 3′-end processing of IGF2BP1 mRNAs is unaltered in aggressive cancers and tumor-derived cells although IGF2BP1 synthesis was proposed to escape let-7 attack by APA-dependent (alternative polyadenylation) 3′ UTR shortening. However, the expression of the triangle factors is inversely correlated with let-7 levels and promoted by LIN28B impairing let-7 biogenesis. Moreover, IGF2BP1 enhances the expression of all triangle factors by recruiting the respective mRNAs in mRNPs lacking AGO proteins and let-7 miRNAs. This indicates that the downregulation of let-7, largely facilitated by LIN28B upregulation, and the protection of let-7 target mRNAs by IGF2BP1-directed shielding in mRNPs synergize in enhancing the expression of triangle factors. The oncogenic potential of this triangle was confirmed in ovarian cancer (OC)-derived ES-2 cells transduced with let-7 targeting decoys. In these, the depletion of HMGA2 only diminishes tumor cell growth under permissive conditions. The depletion of LIN28B and more prominently IGF2BP1 severely impairs tumor cell viability, self-renewal and 2D as well as 3D migration. In conclusion, this suggests the targeting of the HMGA2-LIN28B-IGF2BP1 triangle as a promising strategy in cancer treatment.

INTRODUCTION

MicroRNAs (miRNAs) are small (∼21–23 nt) non-coding RNAs regulating gene expression by inhibiting mRNA translation and/or inducing mRNA decay (1). They play a crucial role in various biological processes and have been implicated in several human diseases, including tumorigenesis.

The let-7 family of miRNAs was first discovered in the nematode *C. elegans* (2) and presents the largest known family of miRNAs with conserved roles in development and diseases (3). In tumorigenesis, the let-7 family is considered to act in a tumor-suppressive manner since it interferes with the expression of various oncogenes or oncogenic factors, respectively. Let-7b gain-of-function screening analyses in tumor-derived cells identified a severe downregulation of various factors (4). The most striking deregulation in two cell lines derived from distinct cancers, liver (HepG2) and lung (A549) cancer, was observed for the architectural transcription factor HMGA2 and the RNA-binding proteins LIN28B and IGF2BP1 (4).

HMGA2 is a member of the High Mobility Group A class of proteins which bind to AT-rich DNA stretches and modulate gene expression by introducing structural alterations in the chromatin landscape. HMGA2-deficiency has been reported to impair growth in mice whereas the transgenic expression of HMGA2 variants enhanced the formation of benign tumors indicating that HMGA2 confers a growth advantage and thus promotes tumorigenesis (5). In agreement, HMGA2 expression is frequently upregulated in cancer, mostly (not exclusively) in tumors of mesenchymal origin (5). This upregulation was reported to involve the down modulation of let-7 directed inhibition of HMGA2 protein synthesis (6,7).

*To whom correspondence should be addressed. Tel: +49 345 552 2860; Fax: +49 345 552 2894; Email: stefan.huettelmaier@medizin.uni-halle.de
†These authors contributed equally to this work as the first authors.

LIN28A/B (lin-28 homologues A/B) negatively regulate let-7 biogenesis by interfering with miRNA processing from let-7 precursors resulting in poly-uridylation and finally let-7 degradation (8,9). LIN28A/B upregulation was reported in various cancers originating from distinct germ layers (10). The transgenic expression of LIN28B induces liver tumorigenesis as well as the formation of neuroblastoma in mice supporting its broad oncogenic potential (11,12). Consistent with their potency in suppressing let-7 biogenesis, LIN28A/B enhance the expression of various oncogenes and were thus suggested to promote the self-renewal potential, proliferation, invasiveness as well as immune escape of tumor cells (10).

IGF2BPs (IGF2 mRNA binding proteins) comprise a family of three mainly cytoplasmic RNA-binding proteins. IGF2BP1 and IGF2BP3 are *bona fide* oncofetal proteins with high expression observed during embryogenesis and severe upregulation or *de novo* synthesis in various tumors (13,14). With the exception of reproductive tissue (15), IGF2BP2 is the only family member present in the adult organism and was implicated in type 2 diabetes (T2D) based on genome wide association studies (16). The let-7 family of miRNAs was shown/suggested to regulate the expression of all three IGF2BP family members and is inversely correlated with the abundance of IGF2BPs in various mouse and cell models (14). In LIN28B-driven liver cancer models, IGF2BP1/3 were proposed as key downstream effectors modulating the self-renewal potential of tumor cells (11). In support of this, the roles of LIN28A/B in controlling the metabolism and growth of stem cells partially rely on the modulation of let-7 dependent regulation of IGF2BP expression (17). Although let-7 dependent regulation was reported/suggested for all IGF2BPs, IGF2BP1 is of special interest. IGF2BP1's 3′ UTR (3' untranslated region) length is controlled by alternative polyadenylation (APA), and the shortening of the IGF2BP1 3′ UTR (maximum length ∼6.7 kb) was shown to abolish let-7 directed regulation. Accordingly, APA was suggested to mediate the upregulation of IGF2BP1 expression in aggressive cancers (18). In addition to the extensive miRNA-dependent regulation of their expression, IGF2BPs also modulate miRNA action on some of their target mRNAs. Reported examples of this regulation are: (i) the inhibition of miR-183 directed downregulation of BTRC1 by IGF2BP1 (19); (ii) the role of IGF2BP1 in antagonizing the downregulation of MITF by miR-340 by IGF2BP1 (20); (iii) the impairment of let-7 dependent downregulation of HMGA2 by IGF2BP3 (21). In all these cases IGF2BPs were shown to enhance the expression of oncogenic factors by interfering with miRNA-targeting.

Intrigued by these observations we set out to evaluate the potency of IGF2BP1 in antagonizing the tumor-suppressive roles of the let-7 family, in particular the downregulation of HMGA2 and LIN28B. In this context, it had to be addressed if the shortening of IGF2BP1's 3′ UTR by APA is indeed essential to direct IGF2BP1 upregulation in primary cancer and tumor-derived cells. Unexpectedly, our studies revealed that the 3′-end processing of IGF2BP1 transcripts appears unaltered in tumor-derived cells as well as primary cancers. Most notably, however, upregulated expression of IGF2BP1 was not associated with 3′ UTR-shortening. However, IGF2BP1 sustains the expression of itself, LIN28B and HMGA2 by recruiting these let-7 target mRNAs in mRNPs lacking let-7 miRNAs and AGO2 protein. Thus, IGF2BP1 shields these transcripts from let-7 attack indicating that IGF2BP1, LIN28B and HMGA2 form a partially self-sustaining oncogenic triangle. The sequestering of the let-7 miRNA family by tough decoys identified distinct roles of the triangle factors in tumor cells. Whereas HMGA2 enhances cell growth under permissive growth conditions, IGF2BP1 and LIN28B are essential to promote the migratory and self-renewal potential of ovarian cancer (OC) cells.

MATERIALS AND METHODS

Plasmids and cloning

Plasmid generation including the respective templates, vectors, restriction sites and oligonucleotide sequences and cloning strategies are summarized in Supplementary Table S4. All PCR (polymerase chain reaction) amplified inserts were sequenced before subcloning in the respective vectors.

miTRAP experiments, small RNA sequencing and data analyses

miTRAP experiments using wild-type (WT) or mutant 3′ UTRs of IGF2BP1, LIN28B and HMGA2 or MS2 as background control as well as sequencing of trapped miRNAs and data analyses were essentially performed as described recently (34). A brief description is provided in the Supplementary materials and methods section.

Sucrose gradient centrifugation and RNA-Immunoprecipitation

Sucrose gradient centrifugation and RNA-Immunoprecipitation were essentially performed as recently described (42,44). A brief description is provided in the Supplementary materials and methods section.

RNA isolation and RT-qPCR

RNA isolation and quantitative RT-PCR (RT-qPCR) were essentially performed as recently described (22,44). In brief, total RNA extracted using Trizol served as template for cDNA synthesis by random priming. RT-qPCR was performed based on SYBRgreen I technology using SYBR Select Master Mix (Life Technologies) in a 7900HT-cycler (Applied Biosystems). Whenever possible, primer pairs spanning an exon/exon border were selected using the Primer Blast database (http://www.ncbi.nlm.nih.gov/tools/primer-blast/). For non-exon-border spanning primer pair, no-RT controls were performed. For all primer pairs an annealing temperature of 58°C in a three step protocol was used. Relative changes of RNA abundance were determined by the ΔΔCt method using ACTB and GAPDH for normalization, as previously described (44). For primers used see Supplementary Table S5.

Northern blotting

Northern blot analyses for the detection of mRNAs or small RNAs were essentially performed as previously described (62,63). A brief description of the important steps is

provided in the Supplementary materials and methods section.

Western blotting and luciferase reporter assays

Infrared Western blotting analyses were performed as previously described (22). Primary antibodies are indicated in Supplementary Table S7. For luciferase reporter assays 1×10^5 ES-2 cells were transfected with 100 ng of pmiR-Glo plasmids or co-transfected with 50 nM miRNA mimics and 100 ng reporter plasmids, as previously described (44). Luciferase activities were determined 36 h post-transfection using DualGlo (Promega). All measurements were performed in triplicates. Firefly luciferase (FFL) activities were normalized by Renilla (RL) activities yielding relative activities (RLU). An empty vector containing the multiple cloning site only (MCS) served as negative control where indicated. RLU ratios were normalized to control populations where indicated.

Deep sequencing analyses and databases

Publically available sequence alignment data files (.bam) of 45 OC cell lines sequenced in context of the cancer cell line encyclopedia (CCLE) (24) were downloaded from the Cancer Genomics Hub (https://cghub.ucsc.edu/). Cell lines and data identifiers are summarized in Supplementary Table S3. Data processing and further analyses are in detail described in the Supplementary materials and methods section.

Where indicated publicly available data were analyzed using the R2 platform (R2: Genomic Analysis and Visualization Platform, link: http://hgserver1.amc.nl/cgi-bin/r2/main.cgi) or SEEK platform (SEEK: Search-Based Exploration of Expression Compendium, link: http://seek.princeton.edu/index.jsp, (51)). Besides a global analyses over all data sets of the R2 database, the CCLE data set consisting of 917 cancer-derived cell lines of different origin (24) as well as two primary cancer data sets (OC—Pamula Pilat—101 samples (64); Neuroblastoma—Versteeg—88 samples (65)) were used.

Cell culture, transduction and transfection

All cell lines used were cultured in Dulbecco's Modified Eagle Medium (DMEM) supplemented with 10% fetal bovine serum (FBS) at 37°C and 5% CO_2. Stably transduced ES-2 cell populations were generated by lenti-viral infection, essentially as previously described (44). Infection efficiency was determined based on GFP expression using MACSQuant (Miltenyi Biotec). All populations used were confirmed to contain >99% GFP-positive cells. For CRISPR/Cas9 directed IGF2BP1 knockout ES-2 cells were transfected with IGF2BP1-KO plasmids encoding Cas9 together with respective sgRNAs were, as previously described (66), using Lipofectamine 2000.

ES-2 cells were transiently transfected with 15 nM of indicated siRNA pools (Supplementary Table S8) to minimize RNAi off-target effects (67). Lipofectamine RNAiMax (Life Technologies) was used in a reverse transfection protocol (6×10^5 cells, 9 μl of RNAiMax in 6-well format). 24 h after transfection cells were transferred in new culture plates and analyzed as described.

Cell growth, spheroid and self-renewal assays

For the assessment of cell proliferation in 2D cultures, 5×10^4 cells were plated 24 h post- transfection and cell number as well as propidium iodide-positive cells were determined by flow cytometry after culturing for an additional 48 h in DMEM+10% FBS. Additionally the 'cell viability' was determined by CellTiter-Glo assays (Promega), essentially as previously described (26).

For spheroid growth analyses 2×10^3 cells (per 96-well) were used in the cultrex spheroid growth assays (Trevigen) according to the manufacturer's instructions using DMEM+10% FBS. Cells were seeded in round-bottom ultra-low attachment plates (Corning) 24 h post-transfection, centrifuged at 300 g for 3 min. Spheres were grown for additional 96 h before bright-field images were acquired using a Nikon TE-2000-E microscope equipped with a live chamber and 4x magnification. The spheroid size was automatically assessed using the Nikon NIS-Elements software measurement tool. Additionally, spheroid viability was determined by the CellTiter-Glo assay (Promega).

To determine the anoikis-resistance and self-renewal potential, 1×10^3 cells were seeded in DMEM/wo FBS per flat bottom ultra-low attachment 96-well (Corning). Cells were cultured for 5 days before documenting spheroid formation by bright-field imaging (see above) and determining cell viability by CellTiter-Glo assays (Promega). For each condition and experiment 8 replicates were analyzed.

Immunofluorescence, migration and microscopy

For immunofluorescence analyses, cells were grown on glass coverslips, fixed and processed using indicated antibodies (Supplementary Table S8), essentially as previously described (44,68). Image acquisition was performed on a Leica SP5X confocal microscope equipped with a white light laser and hybrid detectors using a 63x Plan Apo objective and standardized settings for sequential image acquisition. Representative images are shown.

For 2D single cell migration analyses, cells were seeded on collagen I-coated 8 well chamber slides (IBIDI). For the analysis of single cell migration in 3D, cells were embedded in collagen I matrix at a final concentration of 4 mg/ml (Merck Millipore). Cell spreading was allowed over night before migration was monitored over 10 h by time lapse analyses (2D: 5 min/frame; 3D: 10 min/frame) based on ZsGreen-fluorescence using a Leica SP5X inverse confocal microscope microscope equipped with a Ludin cube life chamber, 20x dry objective and multi-positioning. For analyses of 3D cultures for each position and time point z-stacks were acquired and maximal projections were analyzed. Automated cell tracking was performed using the 'CellMigrationAnalyzer' tool of the MiToBo (http://www2.informatik.uni-halle.de/agprbio/mitobo/) package for ImageJ (http://imagej.nih.gov/ij/) to determine the mean speed [μm/min] of those single cells observed over a time period of at least 2h. A total of 50–100 cells per condition of three different experiments were analyzed.

RESULTS

The let-7 miRNA family is an essential modulator of IGF2BP1 expression in tumor-derived cells

Aiming to characterize the role of let-7 regulated expression of IGF2BPs in cancer-derived cells, the abundance of IGF2BP proteins and let-7 miRNAs was analyzed in a panel of cell lines derived from diverse primary cancers. HEK293A cells served as non-tumor controls expressing all IGF2BPs with exceedingly high levels observed for IGF2BP1 (22,23). Consistent with recent reports (22), IGF2BP1 was absent (BxPC-3) or barely (HCT-116 and MCF-7) expressed in epithelial-like tumor cells (grey) characterized by the expression of e-cadherin (CDH1) and absence of vimentin (VIM; Figure 1A and Supplementary Figure S1A). On the mRNA level, this was further supported in the CCLE comprising microarray expression data of 917 tumor-derived cell lines (24). IGF2BP1 expression was significantly and positively correlated with the expression of VIM and negatively associated with the expression of CDH1 (Supplementary Figure S1B). This was less striking for the other IGF2BPs (Supplementary Figure S1B).

Northern blotting revealed that let-7a is expressed at varying levels in the tumor cell panel with strikingly low levels observed in HEK293A cells and comparatively high levels in the three epithelial-like tumor-derived cells (Figure 1A, lower panel). These findings suggested that the let-7 family essentially controls the expression of IGF2BP1 and possibly also the other IGF2BPs. However, previous studies proposed that the shortening of the IGF2BP1 3′ UTR by APA is essential to escape let-7 directed downregulation in cancer (18). In contrast to IGF2BP2 and IGF2BP3 for which APA has not been shown, three to four IGF2BP1-encoding transcripts with substantially varying 3′ UTR length have been reported (18,25). The shortest IGF2BP1 transcript (S: 2416 nt) lacks let-7 miRNA recognition elements (MREs), the medium sized (M: 3779 nt) contains two and the long variants (L: 8272 or 8769 nt) comprise five validated let-7 MREs (Figure 1B; (18)). In agreement, three major (the large variants are indistinguishable by Northern blotting (18)) IGF2BP1-encoding transcripts were identified by Northern blotting in HEK293A cells but not MCF-7 cells expressing IGF2BP1 at substantially (∼100-fold) lower levels (Figure 1C). Surprisingly, however, the long transcript was the most abundant variant (∼65% of total) in HEK293A cells. This was evaluated in further detail by determining the relative abundance of the long IGF2BP1 transcripts by RT-qPCR in the tumor cell panel (Figure 1D and Supplementary Figure S4D). Similar to HEK293A cells, the longest transcripts were the most abundant variants (in average ∼50% of total), even in epithelial-like tumor-derived cells expressing IGF2BP1 at exceedingly low levels. To determine if the long transcripts substantially contribute to IGF2BP1 protein expression, IGF2BP1 mRNAs were depleted by siRNAs targeting in the distal 3′ UTR (pos. 8429) or coding sequence (CDS, pos.671). OC-derived ES-2 cells were chosen since they express all three IGF2BP paralogues (see Figure 1A) and upregulated expression of all three IGF2BPs was reported to correlate with diseases progression and poor prognosis in OC (26–28). Strikingly, the knockdown of the longest transcripts led to an approximately 2-fold reduction of IGF2BP1 protein abundance whereas protein levels were reduced 10-fold by the siRNA targeting in the CDS (Figure 1E). Hence, the long IGF2BP1 transcript isoforms contributed significantly to IGF2BP1 protein synthesis in ES-2 cells. Together this provided strong evidence that the abundance of let-7 rather than the shortening of IGF2BP1's 3′ UTR by APA is essential for the post-transcriptional control of IGF2BP1 protein synthesis. In support of this, let-7a miRNA abundance was inversely correlated with IGF2BP1 protein abundance in the small panel of tumor cells analyzed (Figure 1A and F) and during mouse brain development (Supplementary Figure S1C and D).

The abundance of let-7 miRNAs is essentially controlled by the RNA-binding proteins LIN28A/B inhibiting let-7 maturation and/or processing, respectively (8). Consistently, we observed that the LIN28B mRNA is the most significantly ($P = 8.3 \times 10^{-23}$) and positively (R = 0.317) correlated transcript of IGF2BP1 in the CCLE comprising expression data of 917 tumor-derived cell lines (Figure 1G; also Supplementary Figure S1J). In contrast, no significant (IGF2BP2) or an only moderate co-expression (IGF2BP3) was observed for the expression of LIN28B and the other IGF2BP family members (Supplementary Figure S1E and F). To test this at the protein level, the expression of IGF2BPs and LIN28B was analyzed in 23 tumor-derived cell lines and HEK293 cells serving as the normalization control (Supplementary Figure S1G–I). This confirmed a significant positive correlation of IGF2BP1 and LIN28B (R = 0.698; $P = 1.48 \times 10^{-4}$) strongly suggesting that IGF2BP1 expression is enhanced by the largely LIN28B-dependent downregulation of let-7 abundance in cancer cells.

The long IGF2BP1 mRNA isoforms are expressed in aggressive cancers

In all analyzed tumor-derived cells the long IGF2BP1 mRNA isoforms were the most abundant transcripts. This suggested that the previously suggested escape from miRNA attack due to the shortening of IGF2BP1's 3′ UTR by APA is largely dispensable for the post-transcriptional upregulation of IGF2BP1 in aggressive cancer.

Initially this was analyzed by RNA-sequencing data of 45 OC-derived cells provided via the CCLE. In 44 cell lines, IGF2BP1 was expressed and the long 3′ UTRs were present (Figure 2A, left panel). Supporting the RT-qPCR analyses, the median sequence coverage indicated that the long transcripts represent ∼50% of all IGF2BP1-encoding transcripts and their expression was significantly correlated with total IGF2BP1 mRNA abundance (Figure 2A, right panel; Supplementary Figure S2B). Aiming to test this in primary OCs by using a distinct technique, the expression of total and long IGF2BP1 transcripts was analyzed in the Anglesio and Bowtell data sets via the R2 database (Figure 2B; (29,30)). Both these data sets are based on Affymetrix (u133plus2.0) microarrays comprising three identifiers for IGF2BP1: (i) 241574_at, that is highly compromised due to alignment with the wrong genomic strand; (ii) 223689_at (short), that identifies a distal region of the coding se-

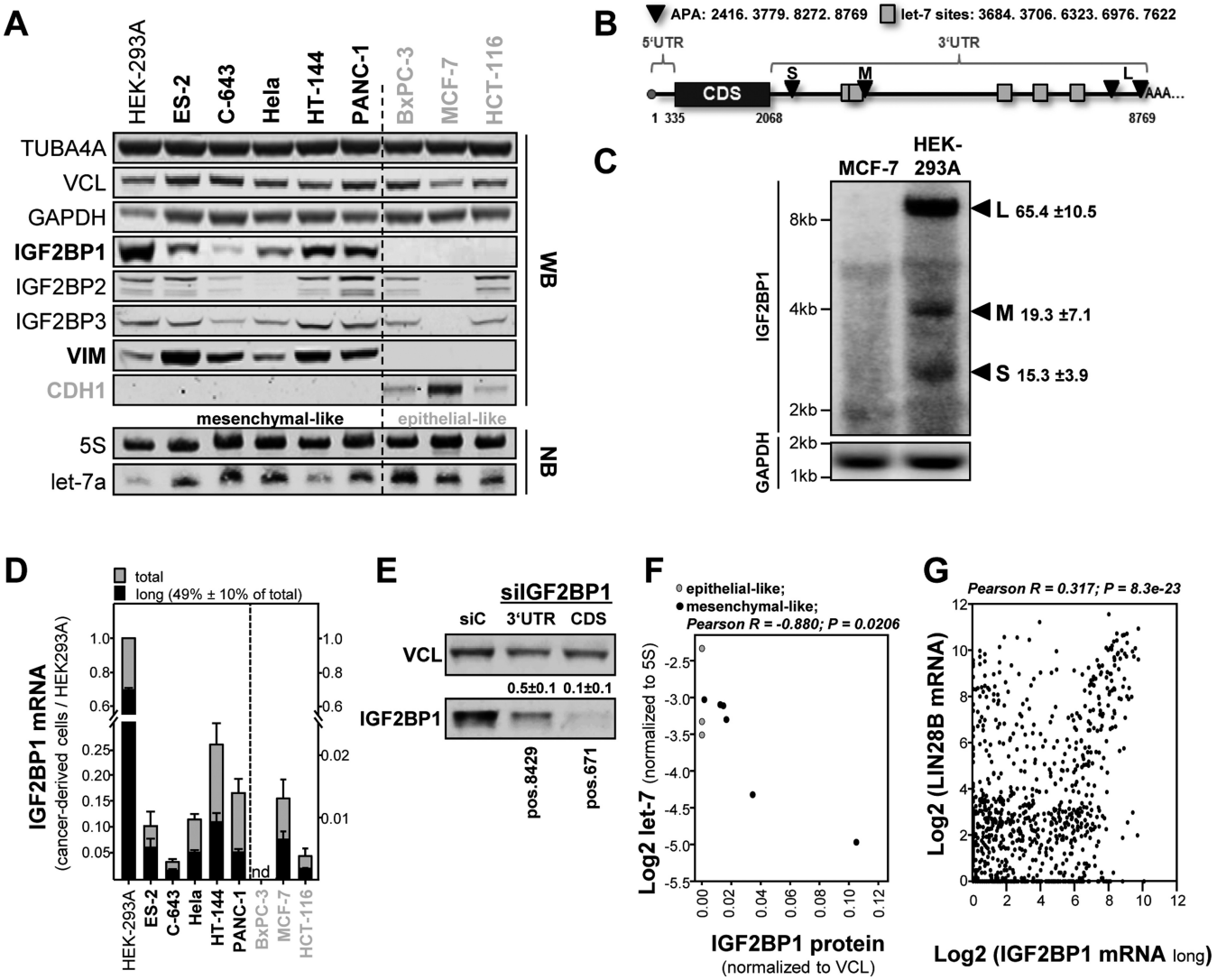

Figure 1. The let-7 miRNA controls the expression of IGF2BP1 in cancer-derived cells largely independent of 3′ UTR shortening by alternative polyadenylation. (**A**) The expression of indicated proteins was analyzed in a panel of mesenchymal- (black, bold) and epithelial-like (green) tumor-derived cells by infrared Western blotting (upper panel; also see Supplementary Figure S1A). The abundance of the let-7a miRNA and 5S rRNA (loading control) was determined by infrared Northern blotting in indicated tumor-derived cells. (**B**) Schematic of IGF2BP1-encoding mRNAs with: (i) reported sites for alternative polyadenylation (APA, black) yielding a short (S), medium-sized (M) and two long (L) transcripts; (ii) let-7 microRNA recognition elements (MREs, green). (**C**) Northern blotting of IGF2BP1 mRNAs in MCF-7 and HEK293A cells using radiolabeled probe covering parts of the coding sequence. GAPDH served as the loading control. (**D**) The relative abundance of the long (black) versus total (grey) IGF2BP1-encoding mRNAs was determined relative to HEK293A cells by RT-qPCR. The dashed line indicates distinct y-axis scaling due to the lack or low IGF2BP1 expression in epithelial-like cells. (**E**) ES-2 cells were transfected with IGF2BP1-directed siRNAs targeting in the distal 3′ UTR (pos. 8429 nt) or coding sequence (pos.671 nt). IGF2BP1 protein abundance was monitored by Western blotting. Vinculin (VCL) served as loading control. (**F**) The 5S rRNA-normalized abundance of the let-7a miRNA (see A) was plotted over VCL-normalized IGF2BP1 protein abundance as determined in (A). Significant inverse Pearson correlation of let-7a miRNA and IGF2BP1 protein is indicated above the graph. (**G**) Significant Pearson correlation (parameters indicated above graph) of LIN28B and IGF2BP1 mRNA expression in the Cancer Cell Line Encyclopedia (CCLE) according to the R2 database.

quence and the most proximal region of the 3′ UTR present in all transcripts; (iii) 227377_at (long), that identifies a distal element of the 3′ UTR observed only in the long mRNA isoforms (Figure 2B, upper panel). Moreover, both data sets were analyzed by the Mas5 normalization and comprise OC samples of all four major FIGO (Federation of Gynecology and Obstetrics) stages. Although signal intensities of the proximal versus distal identifier were positively correlated (Supplementary Figure S2C), increased IGF2BP1 mRNA expression in aggressive (FIGO stages III and IV) tumors was only observed for the distal 3′ UTR identifier (227377_at, grey). This suggests that the proximal identifier underestimates expression. Nonetheless, these findings revealed an upregulation of long IGF2BP1-encoding transcripts and supported previous studies indicating upregulated IGF2BP1 protein expression in aggressive ovarian carcinomas (26). Finally, the expression of IGF2BP1 was analyzed in a third independent OC cohort using semi-quantitative and RT-qPCR (Figure 2C and D). Confirming the microarray data, IGF2BP1 mRNA ex-

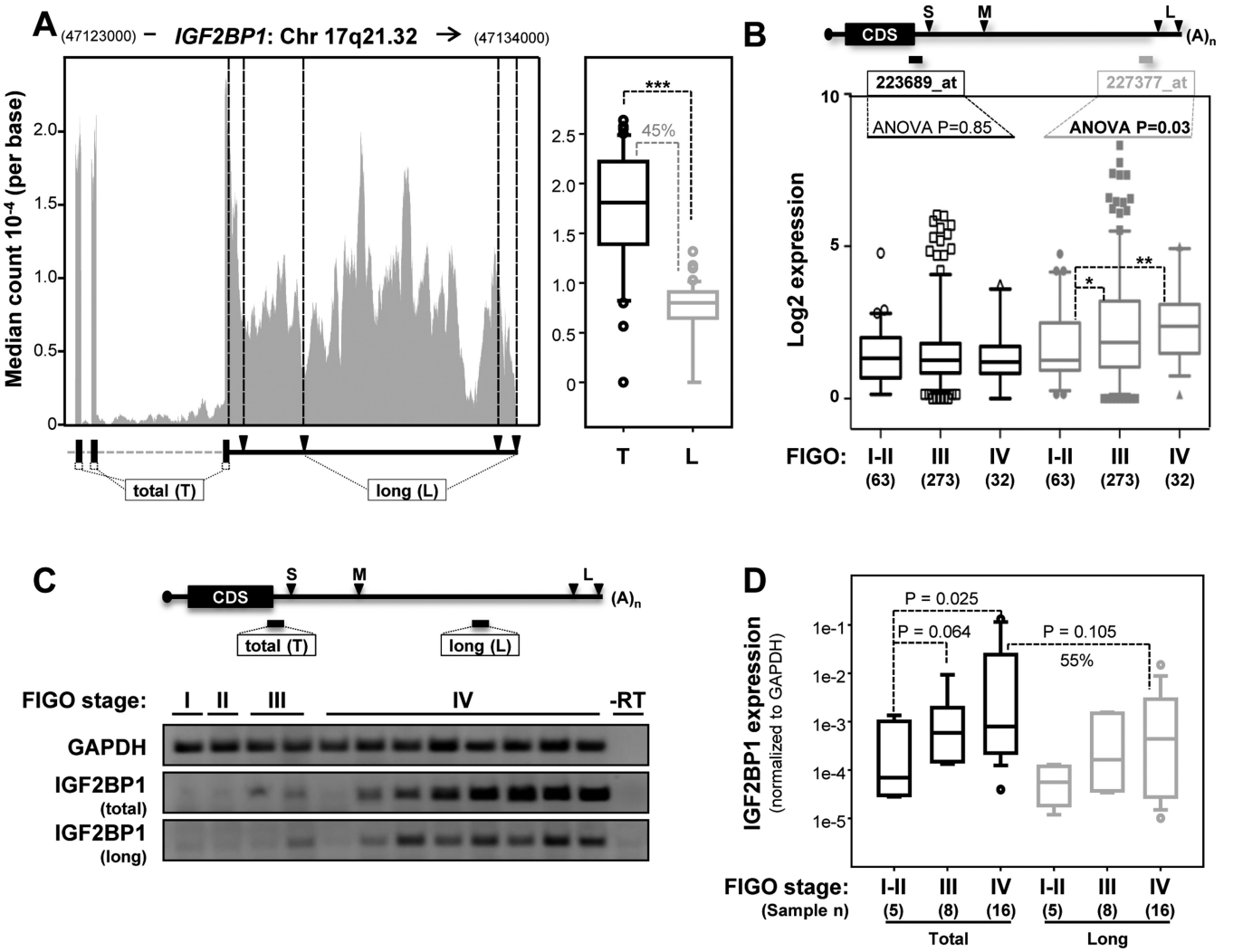

Figure 2. The long IGF2BP1 transcripts are the most abundant IGF2BP1-encoding mRNAs in tumor-derived cells and primary cancer. (**A**) Median read coverage per base determined by RNA-sequencing for the last three exons of IGF2BP1 in 45 ovarian cancer (OC) cell lines analyzed in the CCLE (left panel). The schematic (lower left panel) indicates sequences present in all transcripts (total (T); part of the IGF2BP1 coding sequence) or in the long variants only (long (L)). Black triangles indicate APA-sites. Median read coverage of total (T, black) versus long transcripts (L, grey) determined for each cell line are depicted by box plots (right panel). Cell lines and sample identifiers are indicated in Supplementary Table S3. Statistical significance was determined by a Student's *t*-test: ***$P < 0.001$. (**B**) The schematic (upper panel) shows the longest IGF2BP1-encoding mRNA with APA sites (black triangle) and positions of IGF2BP1-specific identifiers on Affymetrix chips (u133plus2.0). Signal intensities of both IGF2BP1-specific identifiers reported by two OC microarray data sets (Anglesio, n = 90, GSE12172; Bowtell, n = 285, GSE9891) were compared with respect to disease aggressiveness based on FIGO-staging. Statistical significance was determined by ANOVA testing. Notably, intensities of the identifier specific for the long transcript (227377_at) increases with diseases progression. (**C, D**) IGF2BP1 expression in 29 patient samples provided by the gynecological tumor bank (University of Halle) was determined by semi-qRT-PCR (C) and RT-qPCR (D; normalized to GAPDH) with respect to FIGO-staging. Primer pairs used to distinguish the long (L, grey) variants from total (T, black) IGF2BP1 mRNA abundance are indicated in the schematic (C, upper panel). Samples without reverse transcriptase (-RT) served as negative control. Representative samples of all stages are shown (C). Statistical significance was determined by a Rank-Sum-Test. Note that total IGF2BP1 mRNA abundance was increased with higher FIGO-staging and the long transcripts presented ∼55% of total IGF2BP1-encoding mRNAs.

pression was significantly upregulated in aggressive FIGO stage III and IV carcinomas. In all samples with detectable IGF2BP1 mRNA expression, the longest 3′ UTR was observed (Figure 2C). In stage IV tumor samples the long transcripts (grey) represented ∼55% of total IGF2BP1-encoding mRNAs (Figure 2D, black). Moreover, a significant and positive correlation of the long variants with total IGF2BP1 abundance was observed (Supplementary Figure S2D). This was in agreement with the RNA-sequencing analyses of OC cell lines (see Figure 2A), the microarray data analyses of primary OC samples (see Figure 2B) and finally Affymetrix (u133plus2.0) based analyses of 917 tumor cells analyzed in the CCLE (Supplementary Figure S2A). In conclusion, these findings provided strong evidence that 3′ UTR-shortening by APA is negligible for the post-transcriptional upregulation of IGF2BP1 expression in cancer cells and primary OC.

The IGF2BP1 mRNA is a key target of the let-7 miRNA family

Our studies suggested that the post-transcriptional upregulation of IGF2BP1 essentially relies on the downregulation of miRNAs and/or miRNA escape by APA-independent mechanisms. Aiming to characterize the role of miRNAs in the control of IGF2BP1 expression, we analyzed the synthesis of IGF2BP family members in Dicer1 (DCR1) KO-MEFs (mouse embryonic fibroblasts) (31). In these bulk miRNA abundance, including the complete let-7 family, is substantially reduced, as revealed by miRNA-sequencing (Supplementary Figure S3A; Supplementary Table T1). Consistently, IGF2BP1 mRNA and protein levels were significantly upregulated in DCR1 KO-MEFs (Figure 3A; Supplementary Figure S3B). Although less pronounced, this was also observed for IGF2BP2 and IGF2BP3 suggesting that the expression of all IGF2BPs is essentially controlled by miRNAs confirming previous findings (32). To further evaluate the role of let-7 directed regulation of IGF2BP1 expression, the activities of luciferase reporters harboring the longest WT or let-7 MRE-mutated (MUT) 3′ UTRs of IGF2BP1 were analyzed in DCR1 KO-MEFs (Supplementary Figure S3C). As expected, the activity of the WT reporter was significantly upregulated in KO-MEFs. However, the activity of the MUT reporter was modestly yet significantly upregulated as well suggesting that additional miRNAs control IGF2BP1 expression. In support of this, recent studies reported regulation of IGF2BP1 by none let-7 family miRNAs, for instance miR-196b (33).

To identify miRNAs regulating IGF2BP1 expression via the longest 3′ UTR in a comprehensive and quantitative manner we employed the recently established miTRAP (miRNA trapping by affinity purification) protocol (34). To this end *in vitro* transcribed MS2 control RNA, the longest WT or let-7 MRE-mutated (MUT) IGF2BP1 3′ UTRs were used as RNA baits in pulldown analyses (Figure 3B and C). In ES-2 cell lysates both 3′ UTR baits co-purified AGO1 and AGO2 proteins indicating a pivotal role of miRNA-dependent regulation of IGF2BP1 expression (Figure 3D). No binding was observed for the MS2 control or amylose resin loaded with Maltose binding protein-fused MS2-binding protein (MS2BP-MBP). Affinity purification of the bait RNAs was confirmed by syto60-staining of eluted RNAs (lower panel, RNA) and equal loading of the resin was evaluated via MS2BP-MBP. Notably, the association of AGO proteins was significantly reduced for the let-7 MRE-mutated bait RNA (Figure 3D, WT/MUT) and no binding was observed for GAPDH serving as the negative control. This suggested that the let-7 family and/or miRNAs associating at or in proximity of the respective let-7 MREs to present the key but not exclusive regulatory miRNAs controlling IGF2BP1 protein synthesis.

The association of miRNAs with the respective baits was analyzed in further detail by miRNA-sequencing. Selective binding of miRNAs to the WT or MUT baits was determined relative to MS2 controls using TMM (trimmed mean of M-value) normalization and a FDR threshold of 0.05 for differential expression (DE), as previously described (34). This confirmed selective enrichment of let-7 miRNAs with the WT but not the MUT bait (Figure 3E and F; Supplementary Table S2). Only one let-7 family member (let-7g) was still modestly enriched with the mutated 3′ UTR. In total, 87 miRNAs (4.3% of 2042 miRNAs considered) were enriched with the WT versus 75 miRNAs (3.7%) selectively co-purified with the MUT bait RNA (Figure 3G). The number of selectively associating miRNAs remained largely unaffected by mutation of the let-7 MREs, as indicated by 58 (WT: ∼67% of total; MUT: ∼77% of total) miRNAs associated with both baits. However, the quantitative assessment of miRNAs selectively enriched with the wild type 3′ UTR showed that ∼60% of the reads identified members of the let-7 family (Supplementary Figure S3D). Consistently, the size of miRNA libraries generated from RNA co-purified with the MUT bait where reduced by ∼60% compared to WT bait analyses. Importantly, the let-7 family presents only ∼5% of all miRNAs observed in ES-2 cells providing further evidence that miTRAP is not biased by miRNA abundance, as previously shown for the MYC 3′ UTR (34). In addition to the let-7 family, miR-196b-5p and miR-625, previously reported to control IGF2BP1 expression in cancer cells (33,35), were selectively co-purified with the IGF2BP1 3′ UTR (Supplementary Table S2). Notably, the IGF2BP1-targeting miRNAs, miR-494, miR-372 and miR-872 were not expressed in ES-2 cells (36–38).

To evaluate if miRNAs selectively co-purified with the IGF2BP1 3′ UTRs also control IGF2BP1 expression via IGF2BP1's 3′ UTR, four candidate miRNAs identified by miTRAP and let-7d, serving as the positive control, were chosen for further investigations. The transfection of let-7d miRNA mimics severely reduced the activity of the WT-3′ UTR harboring luciferase reporter whereas the let-7 MRE-mutated reporter remained unaffected (Figure 3H). All four miTRAP-identified candidate miRNAs modestly reduced the activity of the WT-reporter indicating their potential to regulate IGF2BP1 expression via the longest 3′ UTR. The *in silico* prediction of putative MREs for the novel IGF2BP1-regulatory miRNAs by miRANDA suggested multiple candidate MREs for miR-17–5p and miR-24–3p (Supplementary Figure S3E). The three validated miR-196–5p MREs overlapped with let-7 targeting sites (Supplementary Figure S3E, red; (33)). Consistently, the activity of the MUT-reporter remained essentially unaffected by the overexpression of this miRNA. Only one out of six predicted miR-17–5p targeting sites overlapped with let-7 MREs. In agreement, the activity of both reporters was downregulated by miR-17–5p. For miR-24–3p only three candidate MREs with one let-7 MRE-overlapping site were predicted. Although WT-reporter activity was downregulated by miR-24–3p, the MUT-reporter remained essentially unaffected suggesting this miRNA to target mainly via the let-7 MRE-overlapping site. Only for miR-181–5p no canonical targeting site could be identified. Accordingly, a putative non-canonical site was determined by RNA-hybrid (Supplementary Figure S3E). This none let-7-overlapping candidate MRE is located in proximity to the stop codon. Consistently, miR-181a-5p regulated both reporters.

Taken together the miTRAP studies revealed that the long IGF2BP1 transcripts are subjected to regulation by multiple miRNAs with the let-7 family presenting the most potent class of regulators. The reporter analyses, moreover

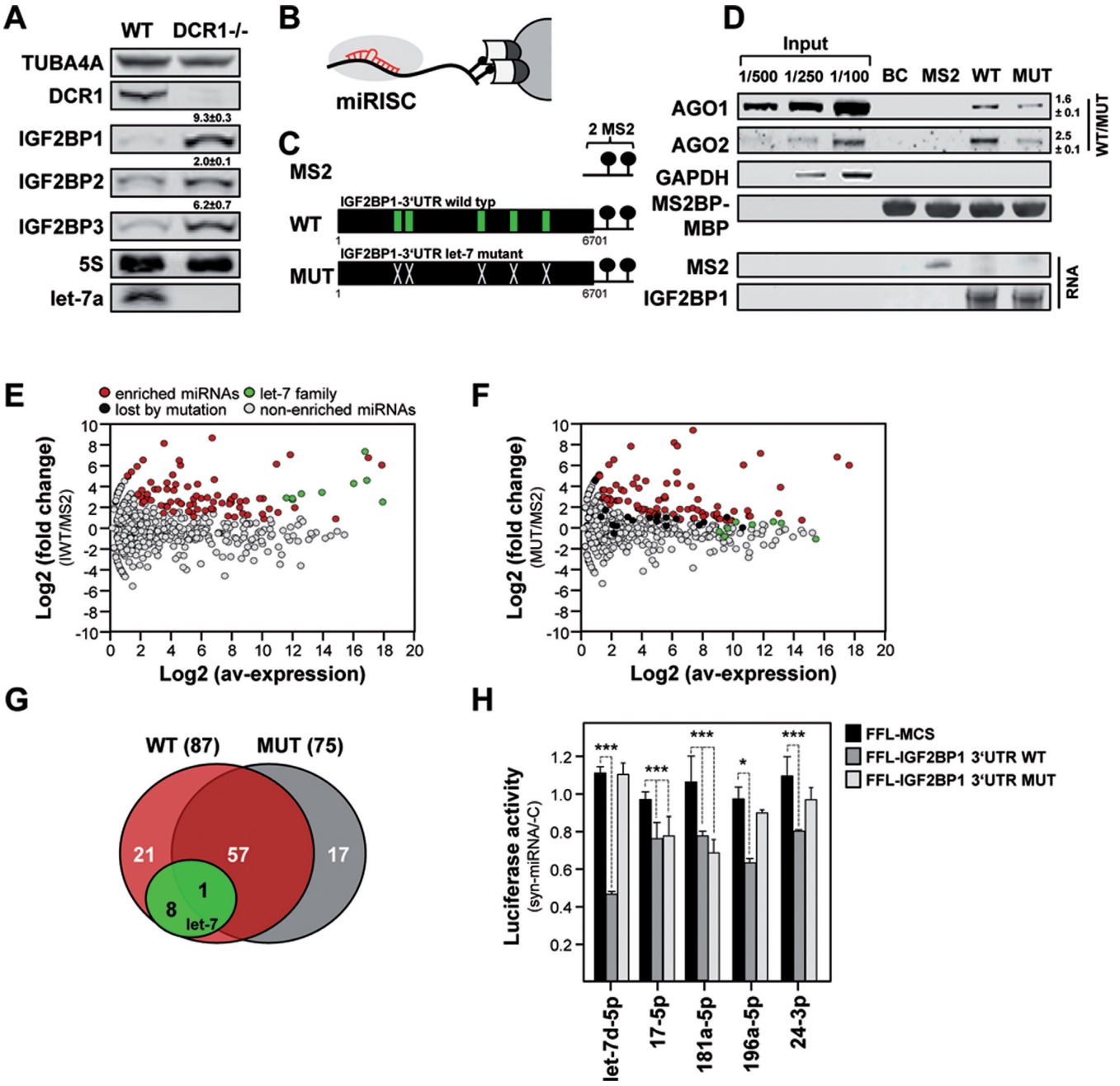

Figure 3. The let-7 miRNA family is the most potent among various IGF2BP1-regulatory miRNAs. (**A**) The expression of indicated proteins and the let-7a miRNA was determined in wild-type (WT) and DCR1 (-/-) MEFs by infrared Western or Northern blotting, respectively. TUBA4A protein and 5S rRNA served as loading controls. The fold change of IGF2BP proteins in DCR1 (-/-) MEFs is indicated. Errors indicate standard deviation over three independent studies. (**B**) Schematic of the miTRAP method identifying regulatory miRNAs by RNA-affinity purification using MS2-thethering, essentially as recently described (34). (**C**) Schematics of RNA baits used for miTRAP analyses with MS2 aptamers and 2xMS2-containing IGF2BP1 WT or let-7 MRE-mutated (MUT) 3′ UTR baits. Let-7 MREs are indicated by green boxes in WT. (**D**) Western blotting of indicated proteins (upper panel) or Syto60-stained PAGE gels indicating affinity purified RNA baits (lower panel) in miTRAP elutes. (**E** and **F**) Scatter plot depicts the log fold change (FC) of miRNA enrichment determined by a Poisson exact test for the WT or MUT baits in ES-2 cells over the averaged TMM-normalized logCPM of miRNA reads in inputs. MiRNAs significantly enriched with the respective baits (FDR < 0.05, colored), the let-7 miRNAs (green) as well as miRNAs only enriched with the WT bait (black) are indicated. (**G**) Pie chart indicating miRNAs selectively co-purified with only one or both of the used IGF2BP1–3′ UTR baits. The let-7 family is highlighted in green. (**H**) The activity of Firefly luciferase reporters comprising the longest wild type (WT, dark grey), let-7 MRE-mutated (MUT, light grey) 3′ UTRs of IGF2BP1 or only the pmiR-Glo encoded MCS (MCS, black) was determined in ES-2 cells transfected with indicated miRNA mimics. The Renilla luciferase-normalized activity of reporters was determined relative to controls co-transfected with a control miRNA (cel-239b-5p). Error bars indicate s.d. of at least three independent analyses. Statistical significance was determined by a (two-sided) Student's *t*-test: $*P < 0.05$; $***P < 0.0005$.

suggested that let-7 MREs serve as essentially hubs for miRNA-dependent regulation.

Let-7 miRNAs are key regulators of IGF2BP, LIN28B and HMGA2 expression in cancer cells

The correlation of let-7 abundance with the expression of IGF2BP1 transcript isoforms in cancer (see Figures 1 and 2) and the miTRAP studies (see Figure 3) confirmed that IGF2BP1 is a major downstream target of let-7 in cancer, as previously proposed (4). Accordingly, we hypothesized that the previously reported tumor-suppressive role of the let-7 family is essentially modulated by the downregulation of IGF2BP1 expression. To characterize the potency of the let-7/IGF2BP1 axis in determining tumor cell fate, lentiviral vectors encoding let-7 directed though decoys were established (Figure 4A).

In ES-2 cells stably transduced with the let-7 directed decoy (TuD-let-7) the activity of let-7a, let-7d and let-7i antisense luciferase reporters was significantly (∼3-fold) upregulated indicating a substantial and ample impairment of let-7 directed regulation (Figure 4B; Supplementary Figure S4A). Consistently, the expression of IGF2BP1 as well as other reported let-7 targets including IGF2BP paralogues (14,32,39), HMGA2 (6) as well as LIN28B (4) was severely upregulated at the protein and mRNA level (Figure 4C and D). This increase in let-7 target gene expression was positively and significantly correlated with the number of let-7 MREs in the respective target mRNAs (Figure 4E and F; note that two additional sites were identified for LIN28B on the basis of *in silico* predictions). Moreover, the activity of WT but not let-7 MUT luciferase reporters harboring the 3′ UTRs of IGF2BP1, HMGA2 or LIN28B was selectively increased by TuD-let-7 in a MRE number-dependent manner (Figure 4G).

To test if let-7 dependent regulation of IGF2BP1, LIN28B and/or HMGA2 is also observed in other OC-derived cells, their protein expression was analyzed along with let-7a miRNA abundance (Supplementary Figure S4B). In the OC-derived cells, the expression of all three factors appeared inversely correlated with let-7a miRNA abundance. Notably, the expression of all three factors increased with the proposed aggressiveness of the analyzed OC-derived cell lines, as determined by genomic profiling (40). The highest expression of all three factors was determined in hepatocellular carcinoma (HCC) derived Huh7 and OC-derived COV318 cells, in which let-7a was not or barely observed by Northern blotting (Supplementary Figure S4B). Consistently, let-7a as well as let-7i anti-sense luciferase reporter activity was substantially increased with decreased let-7 miRNA expression (Supplementary Figure S4C). RT-qPCR analyses revealed the presence of the long IGF2BP1 3′ UTR in all cell lines (∼50% of total IGF2BP1-encoding transcripts) for which expression was observed providing further evidence that shortening of the IGF2BP1 3′ UTR is not associated with upregulated expression of IGF2BP1 in cancer-derived cells (Supplementary Figure S4D). The expression of IGF2BP1, LIN28B and HMGA2 (if detectable in parental cells) as well as let-7 anti-sense luciferase reporter activity were increased by the let-7 family directed decoy vector in all OC-derived cells analyzed (Supplementary Figure S4E and F). These findings confirmed the pivotal role of the let-7 miRNA family in the post-transcriptional regulation of HMGA2, LIN28B and IGF2BP1 expression. Let-7 decoy directed upregulation was most prominent in ES-2 cells indicating the latter as the most suitable test model for analyzing the role of the let-7 family in modulating the expression of all three factors in OC-derived tumor cells (compare Figure 4C and Supplementary Figure S4E).

IGF2BP1 impairs let-7 directed downregulation of HMGA2, LIN28B and itself

In previous studies others and we demonstrated that IGF2BP1 associates with target mRNAs in cytoplasmic mRNPs (41,42) and thereby modulates target mRNA translation (25,43,44), shields associated transcripts from nucleolytic cleavage (42) and/or miRNA-targeting (19). The latter suggested that IGF2BP1 is not only targeted by the let-7 family of miRNAs but also interferes with let-7 directed regulation by shielding associated transcripts from miRNA attack. Notably, this was recently demonstrated for IGF2BP3-dependent control of HMGA2 expression (21).

PAR-CLIP analyses in HEK293 cells identified binding sites for IGF2BP1 in the CDS and/or 3′ UTRs of IGF2BP1 itself, LIN28B and HMGA2 ((45); Supplementary Figure S5A). With the exception of two let-7 MREs in the HMGA2 3′ UTR the reported CLIP-tags for IGF2BP1 did not overlap directly with validated let-7 MREs. In agreement, MS2-tethering studies in ES-2 cell extracts using the longest WT versus let-7 MUT 3′ UTRs of IGF2BP1, LIN28B or HMGA2 showed that IGF2BP1 association was unaffected by the inactivation of let-7 MREs (Supplementary Figure S5B). In contrast, AGO2 co-purification was markedly reduced for all three MRE-mutated RNA baits confirming the pivotal role of let-7 directed regulation and selective copurification of miRNAs and/or RNA induced silencing complexes (RISC), respectively.

To test if IGF2BP1 modulates HMGA2 and LIN28B synthesis, the expression of IGF2BP1 was impaired by CRISPR/CAS9 directed targeting of the *IGF2BP1* locus in ES-2 cells. Although residual IGF2BP1 expression including modestly shortened protein variants, presumably due to alternative translation initiation were observed in the cell population, HMGA2 as well as LIN28B expression were modestly decreased (Supplementary Figure S5C). More strikingly, the re-expression of GFP-IGF2BP1 as well as its chicken ortholog enhanced HMGA2 and LIN28B protein abundance in a dose-dependent manner. Notably, HMGA2 and LIN28B expression was only modestly restored by the re-expression of a RNA-binding deficient mutant of chicken IGF2BP1 (IGF2BP1mut; (46)) providing evidence for the protective role of IGF2BP1-association with the respective transcripts. If this protective role is due to shielding target transcripts from let-7 attack and accordingly also applies to the expression of endogenous IGF2BP1, was analyzed by gain-of-function studies in ES-2 cells. The forced expression of GFP-tagged human and chicken IGF2BP1 orthologs resulted in a RNA-binding and dose-dependent increase in IGF2BP1, HMGA2 and LIN28B protein abundance (Figure 5A and B). This was associated with modestly increased

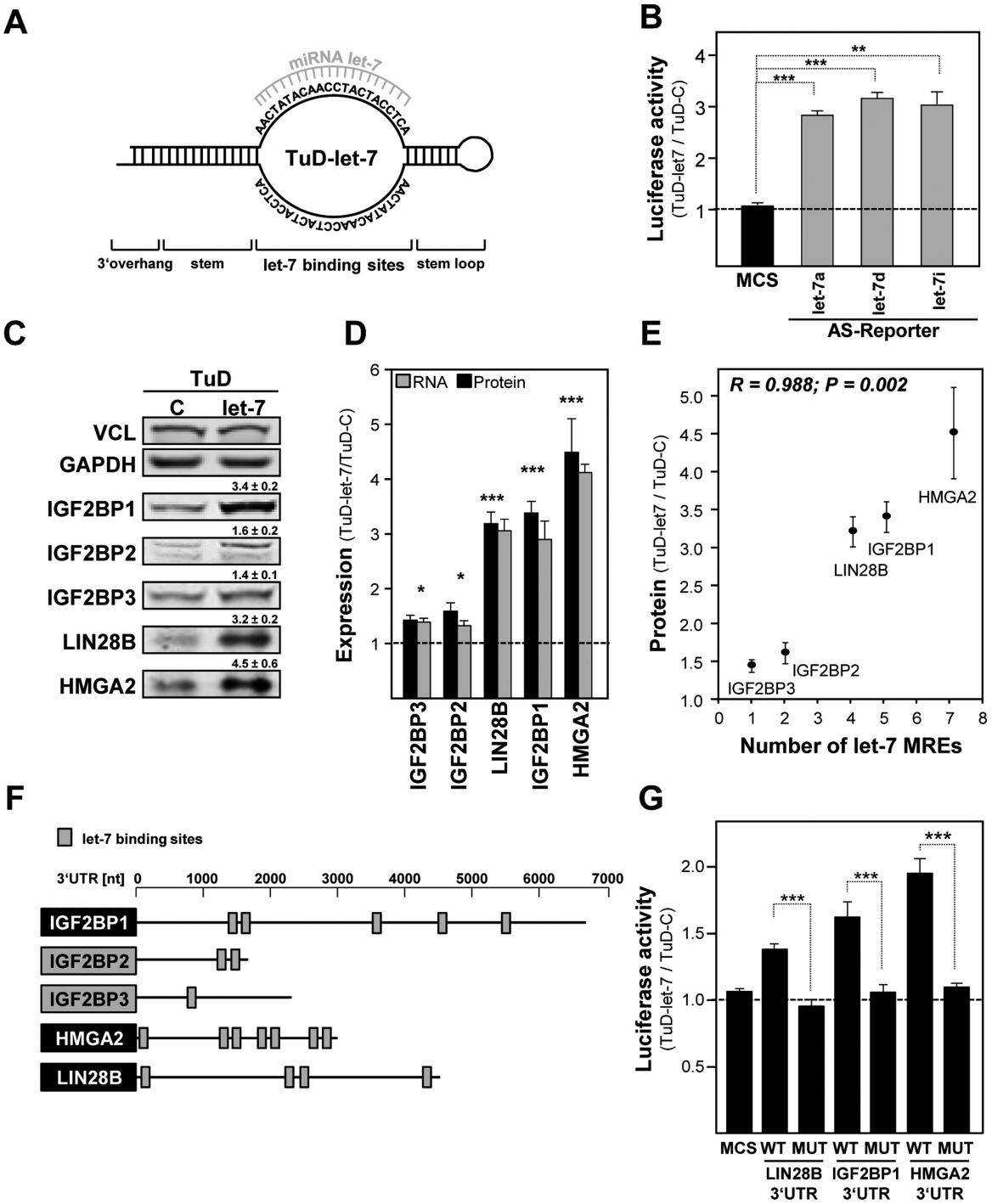

Figure 4. Let-7 directed tough decoys impair the let-7 dependent inhibition of IGF2BPs, HMGA2 and LIN28B. (**A**) Schematic of a tough decoy vector directed against the let-7 family (TuD-let-7) of miRNAs, essentially designed as previously described (61). (**B**) The activity of indicated let-7 antisense Firefly reporters were determined in ES-2 cells stably transduced with TuD-let-7 or control (TuD-C) decoy vectors. The s.d. of Renilla-normalized Firefly activity ratios (TuD-let-7/TuD-C) was determined in three independent studies. (**C**) The abundance of indicated proteins was analyzed in ES-2 cells stably transduced with TuD-C or TuD-let-7. The fold change of protein abundance with s.d. was determined in three independent analyses. VCL protein levels served for normalization. (**D**) The fold change of indicated mRNAs in TuD-let-7 versus TuD-C transduced ES-2 cells was analyzed by RT-qPCR by the $\Delta\Delta C_t$-method using PPIA for normalization. Error bars indicate the s.d. of three independent analyses. (**E**) The plot depicts the fold change of indicated protein abundance in TuD-let-7 versus TuD-C transduced ES-2 cells over the number of validated let-7 MREs in the respective 3′ UTRs of protein-encoding mRNAs. Pearson correlation (parameters indicated in graph) revealed that the fold change in protein abundance is significantly increased with the number of let-7 MREs. (**F**) Schematics of IGF2BP, HMGA2 and LIN28B encoding transcripts with coding sequences (boxes, gene symbol), 3′ UTRs (scale in nucleotides, nt) and let-7 MREs (grey boxes). (**G**) The activity of luciferase reporters comprising the longest WT or let-7 MUT 3′ UTRs of indicated genes or the pmiR-Glo encoded multiple cloning site (MCS) was determined in ES-2 cells stably transduced with TuD-let-7 or TuD-C. Error bars indicate s.d. of at least three independent analyses of Renilla-normalized Firefly activity ratios (TuD-let-7 versus TuD-C). Statistical significance was determined by a (two-sided) Student's *t*-test: $*P < 0.05$; $**P < 0.005$; $***P < 0.0005$.

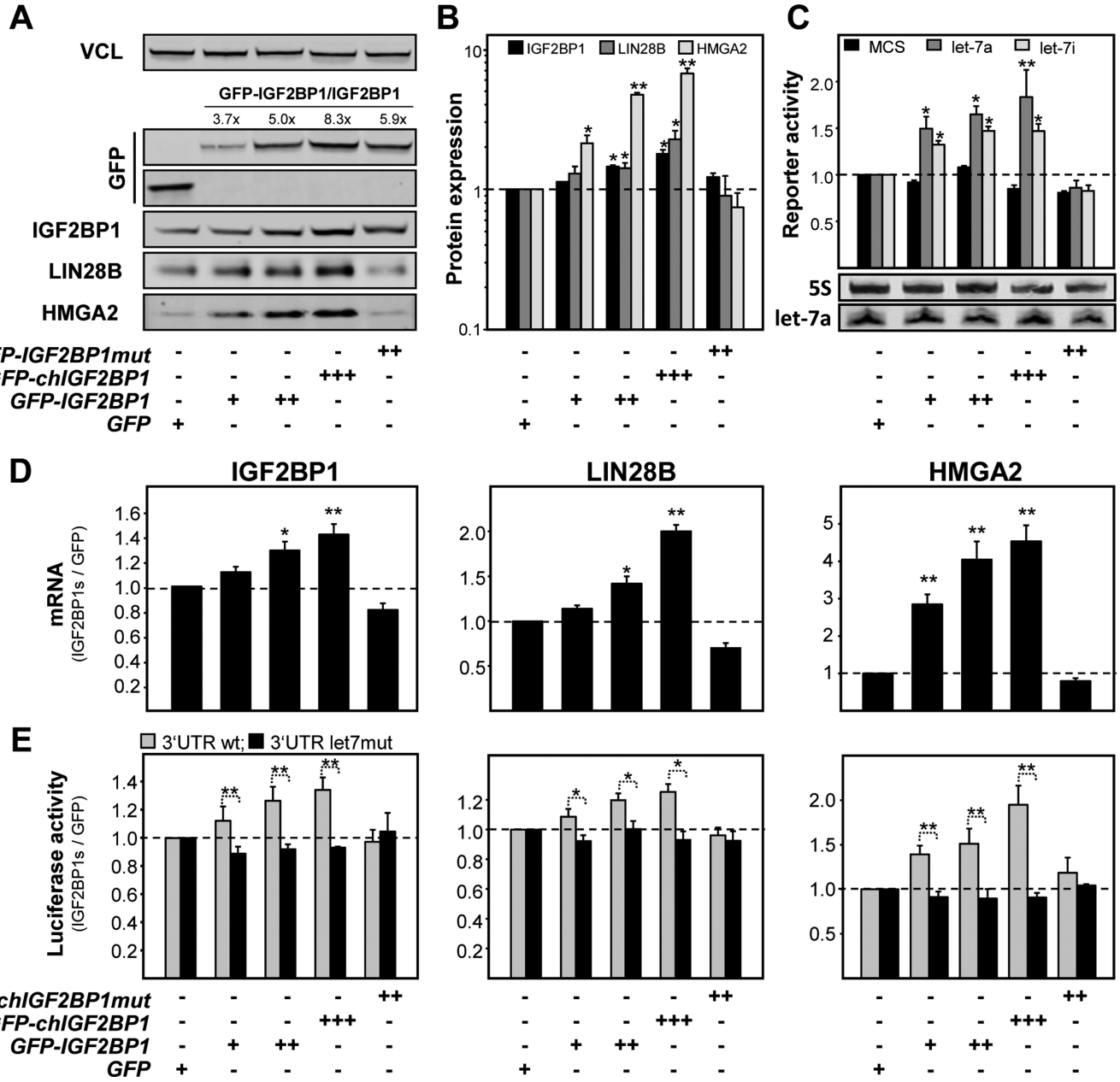

Figure 5. IGF2BP1 shields target mRNAs from let-7 miRNA attack. ES-2 cells were stably transduced with GFP-tagged IGF2BP1 variants or GFP as a control. The GFP-IGF2BP1mut protein (chIGF2BP1) contains mutations in the GXXG loop of all four KH-domains abolishing RNA-binding (46). (**A**) The abundance of indicated proteins (bottom) was analyzed by Western blotting. The fold change of GFP-IGF2BP1 protein variants over endogenous IGF2BP1 levels is indicated. (**B**) The fold change of indicated proteins in IGF2BP1-transduced ES-2 cells was determined relative to GFP-transduced ES-2 cells. (**C**) The fold change in Renilla-normalized Firefly activities of indicated antisense reporters was determined relative to ES-2 control cells transduced with GFP-encoding vectors. Let-7a levels of the same cell populations were determined by Northern blotting (lower panel). 5S served as loading control. (**D**) The abundance of IGF2BP1, LIN28B or HMGA2 mRNAs was determined in ES-2 cells stably transduced with indicated (top, see A–C) GFP-tagged proteins. The fold change of mRNA abundance was determined relative to GFP-transduced controls by the $\Delta\Delta C_t$-method using GAPDH and ACTB for normalization. (**E**) The activity of Firefly reporters comprising the WT (light grey) or let-7 MRE-mutated (black) 3′ UTRs of IGF2BP1, LIN28B or HMGA2 were determined as in (C) in ES-2 cells transduced as indicated (bottom). Errors in all analyses indicate the s.d. determined in at least three independent studies. Statistical significance was determined by a (two-sided) Student's *t*-test: $*P < 0.05$; $**P < 0.005$.

let-7 antisense reporter activity suggesting that upregulated LIN28B expression led to a very modest decrease in mature let-7 levels (Figure 5C, upper panel). This, however, was not veritably detectable by Northern blotting suggesting that IGF2BP1 enhanced the expression of itself, HMGA2 and LIN28B largely independent of impairing let-7 biogenesis through LIN28B (Figure 5C, lower panel).

The levels of all three endogenous mRNAs as well as the activity of luciferase reporters harboring the WT 3′ UTRs of all three transcripts were increased in a RNA-binding and IGF2BP1 protein dose-dependent manner (Figure 5D and E). Importantly, the activity of reporters harboring 3′ UTRs with inactivated let-7 MREs remained essentially unchanged. These findings suggested that IGF2BP1 enhanced the expression of HMGA2, LIN28B and itself by shielding the respective mRNAs from let-7 attack (Figure 5E). This was analyzed further in HCC-derived Huh7 and OC-derived COV318 cells expressing exceedingly high levels of IGF2BP1 but barely any or very moderate levels of let-7 miRNA, respectively (see Supplementary Figure S4B). In both cell lines the abundance of IGF2BP1, HMGA2 or LIN28B proteins remained essentially unchanged by the stable expression of WT GFP-IGF2BP1 (Supplementary Figure S6A). This indicated that the let-7 antagonizing protective role of IGF2BP1 is negligible at very low levels of let-7 miRNAs and high abundance of endogenous IGF2BP1.

To compare the potency of upregulated IGF2BP1 versus HMGA2 or LIN28B expression, all three proteins were stably overexpressed in ES-2 cells (Supplementary Figure S6B and C). GFP-IGF2BP1 enhanced the synthesis of all three endogenous factors to varying extends at the mRNA and protein levels supporting a miRNA-protective role. LIN28B upregulated the expression of all three factors as well. However, compared to IGF2BP1 this enhancement was significantly stronger supporting LIN28B's potency in impairing let-7 biogenesis (data not shown). The forced expression of the architectural transcriptional regulator HMGA2 only led to significantly elevated expression of IGF2BP1. This suggested that HMGA2 stimulated IGF2BP1 mRNA synthesis, as previously shown for its homologue IGF2BP2 (47), or modulated secondary regulation. In summary these findings suggested a powerful self-promoting triangle consisting of HMGA2 acting at the transcriptional level, IGF2BP1 modulating gene expression by shielding mRNAs from miRNA attack and LIN28B that antagonizes let-7 biosynthesis.

IGF2BP1 protects the let-7 target mRNAs IGF2BP1, HMGA2 and LIN28B via RISC-free mRNPs

IGF2BP1 enhanced the expression of itself, HMGA2 and LIN28B in a dose and RNA-binding dependent manner by protecting target mRNAs from let-7 attack. This suggested that the protein recruits the respective let-7 target mRNAs in previously reported cytoplasmic mRNPs devoid of let-7 miRNAs and RISC proteins (41,42,46).

To characterize these putative protective mRNPs, cell extracts of ES-2 cells expressing WT IGF2BP1, the RNA-binding deficient mutant protein or GFP were analyzed by linear (5–20%) sucrose gradient centrifugation (Figure 6A). This allowed the enrichment of pre-polysomal mRNPs comprising mRNA (Figure 6B), endogenous and GFP-tagged wild type IGF2BP1 and 18S rRNA in fraction five (Figure 6A, mRNP). Western and Northern blotting identified barely any AGO2, let-7 miRNAs, GFP or RNA-binding deficient IGF2BP1 in these fractions (Figure 6A). However, compared to GFP or the IGF2BP1 RNA-binding mutant protein expressing cells, the forced expression of GFP-IGF2BP1 resulted in a strikingly elevated abundance of let-7 target mRNAs regulated by IGF2BP1 (Figure 6B, total input; also compare Figure 5D) and their enrichment in fraction five, as determined by GAPDH mRNA normalized RT-qPCR (Figure 6B). In contrast, no enrichment was observed for the PPIA (cyclophilin A) mRNA that is neither associated nor regulated by IGF2BP1 (44). If GFP-IGF2BP1 associated with its target mRNAs and/or RISC components in these complexes was analyzed by the immunopurification of GFP-tagged proteins from fraction five (Figure 6C). Consistent with an only moderate abundance of GFP and the GFP-tagged RNA-binding deficient mutant in fraction five (Figure 6C, mRNP input), only the GFP-tagged wild type IGF2BP1 was significantly enriched by immunoprecipitation. Endogenous IGF2BP1 was co-purified with GFP-IGF2BP1 supporting previous reports on the RNA-dependent oligomerization of IGF2BPs (46). AGO2 protein was not associated with GFP-IGF2BP1 indicating that the mRNPs lack RISC protein components. In agreement, let-7a miRNA was neither observed in inputs (mRNP) nor in immunopurified GFP-IGF2BP1 associated complexes by Northern blotting. This was further supported by RT-qPCR analyses revealing that only ∼0.3% of total let-7a was found in the mRNP fraction but not detectable upon GFP-IGF2BP1 immunopurification (data not shown). Although barely observed in the mRNP input fractions, due to their low abundance (only 5% were used for cDNA synthesis), semi-quantitative RT-PCR demonstrated that all three let-7 and IGF2BP1 target mRNAs were selectively associated with GFP-tagged IGF2BP1. In contrast, the highly abundant GAPDH mRNA (see mRNP input) was not co-purified with GFP-IGF2BP1.

In conclusion, these findings identified pre-polysomal complexes comprising WT IGF2BP1 associated with let-7 target mRNAs. Notably, these complexes lacked AGO2 and let-7 miRNAs suggesting that IGF2BP1 protected target mRNAs from miRNA attack by recruiting target mRNAs in RISC/let-7 devoid mRNPs.

Let-7 impairs tumor cell growth and self-renewal by suppressing the HMGA2-IGF2BP1-LIN28B triangle

The let-7 miRNA family was shown to act in a tumor-suppressive manner in distinct cancers, including OC (48). Aiming to reveal the role of the let-7 antagonizing triangle consisting of HMGA2, IGF2BP1 and LIN28B in directing the phenotypes of OC-derived ES-2 cells, the three proteins were independently depleted by siRNA pools in ES-2 cells stably transduced with the let-7 family directed decoy (Figure 7A). Compared to ES-2 cells transduced with control decoys, the expression of all triangle factors was upregulated by the let-7 directed tough decoy. The depletion of each triangle factor only modestly impaired the other factors, for instance LIN28B and HMGA2 were mildly down-

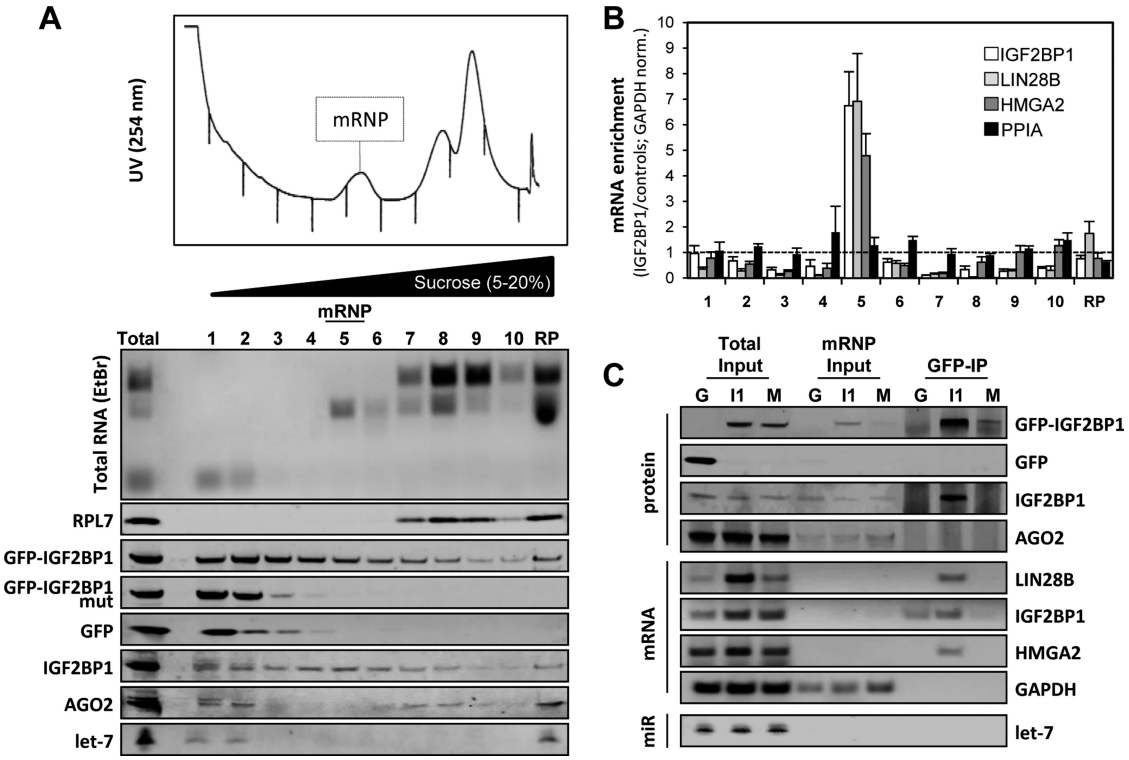

Figure 6. The IGF2BP1-'safe-guard' mRNPs lack miRISC components. (**A**) Pre-polysomal mRNPs were analyzed by linear 5–20% sucrose gradient centrifugation. The UV-254nm profile (top) was recorded for 10 fractions. The distribution of rRNAs was analyzed by ethidium bromide (EtBr) stained agarose gels for all fractions and the ribosomal pellet (RP). The sedimentation of indicated proteins and the let-7a miRNA was monitored by Western and Northern blotting, respectively (lower panel). (**B**) The mRNA enrichment (GFP-IGF2BP1 to GFP and GFP-IGF2BP1 mutant) in each fraction was determined by RT-qPCR using GAPDH for normalization. Ratios were corrected for increased abundance of target mRNAs upon GFP-IGF2BP1 expression via input samples. (**C**) RIP and protein copurification (GFP-IP) analyses of the mRNP fraction isolated from cells stably transduced with GFP (G), GFP-IGF2BP1 (I1) or the GFP-IGF2BP1 KH-mutant (M) were performed using GFP-directed antibodies. Proteins were analyzed by Western blotting with indicated antibodies (protein), mRNAs were monitored by semi-quantitative RT-PCR (mRNA) and let-7a abundance was determined by Northern blotting (miR). Protein and RNA abundance in total input or the mRNP fraction (mRNP input) are indicated on the left. Representative analyses are shown.

regulated by the depletion of IGF2BP1 in the let-7 decoy-transduced cells. This suggested that the experimental set-up provides a suitable approach for testing the role of each factor in antagonizing the 'tumor-suppressive' role of the let-7 family.

In 2D-cultured cells the impairment of let-7 directed regulation led to a significant increase of tumor cell proliferation, as evidenced by increased cell numbers determined by flow cytometry (Supplementary Figure S7A). Cell numbers were significantly reduced by the depletion of IGF2BP1 and HMGA2 but not LIN28B. Notably, the number of dead cells remained essentially unchanged (Supplementary Figure S7B). This showed that the reduction of let-7 activity by TuD-let-7 in 2D-cultured cells led to elevated proliferation through (at least in part) the upregulation of IGF2BP1 and HMGA2. Like observed in 2D-cultured cells, the growth and viability of 3D-cultured ES-2 cell spheroids, grown in concave low adhesion plates, was enhanced by TuD-let-7 and significantly reduced by the depletion of IGF2BP1 or HMGA2 but not LIN28B (Figure 7B and C; Supplementary Figure S7C). Finally, the role of the let-7 antagonizing triangle on anoikis resistance and the self-renewal potential of ES-2 cells was investigated by monitoring spheroid formation and viability in the absence of FBS using planar low adhesion plates (Figure 7D and E). Confirming the tumor-suppressive role of the let-7 miRNA family, the formation and viability of spheroids and cell clusters cultured in the absence of FBS was substantially enhanced. In contrast to analyses performed in FBS-containing medium, the depletion of HMGA2 remained ineffective whereas the knockdown of LIN28B significantly decreased the formation and viability of spheroids. Strikingly, the depletion of IGF2BP1 severely impaired or even abolished spheroid formation and viability.

Taken together these findings indicated that let-7 directed regulation of gene expression impairs the proliferation, self-renewal and anoikis resistance of tumor cells. Under favorable conditions (in the presence of FBS) the anti-proliferative role of the let-7 family was partly facilitated via the impairment of HMGA2 and/or IGF2BP1 expression. Self-renewal and anoikis resistance, however, were largely modulated by let-7 directed downregulation of LIN28B and most strikingly IGF2BP1.

Let-7 impairs tumor cell migration by suppressing IGF2BP1 and LIN28B

In addition to elevated proliferation and renewal capacity an aggressive tumor cell phenotype is commonly charac-

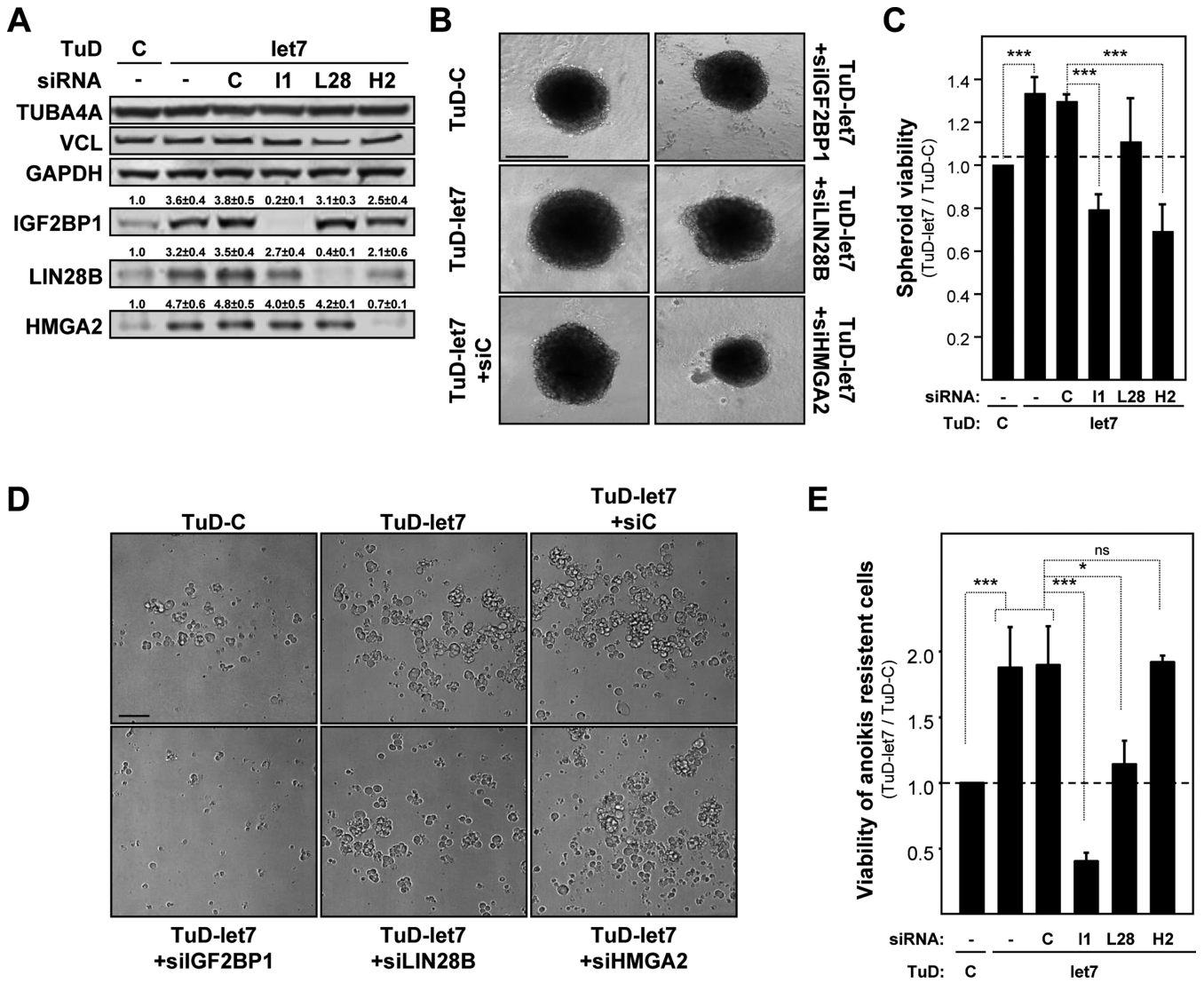

Figure 7. The HMGA2-LIN28B-IGF2BP1 triangle antagonizes let-7 directed repression of tumor cell growth and self-renewal. (**A**) The expression of indicated proteins was analyzed by Western blotting in ES-2 cells stably transduced with control (TuD-C) or let-7 directed (TuD-let-7) decoys upon the transient transfection with indicated siRNA pools for 72 h. The fold change of protein abundance (indicated above lanes) was determined relative to TuD-C transduced non-transfected controls. Errors indicate the s.d. of three independent analyses. (**B** and **C**) Representative images (bar, 500 μm) of spheroids formed in conical low adhesion plates (DMEM/10%FBS, 72 h) by ES-2 cells transduced with decoys and transfected with siRNA pools as indicated were acquired by light microscopy (B). The viability (C) of ES-2 cells in spheroid studies was determined by Celltiter-GLO relative to non-transfected ES-2 cells transduced with control decoys (TuD-C). (**D** and **E**) Representative images (bar, 100 μm) of spheroids formed in planar low adhesion plates (DMEM/woFBS, 120 h) by ES-2 cells transduced with decoys and transfected with siRNA pools as indicated were acquired by light microscopy as in (B). The viability (E) was determined as described in C. Errors indicate the s.d. of at least three independent studies. Statistical significance was determined by a (two-sided) Student's *t*-test: $*P < 0.05$; $***P < 0.0005$; ns $P \geq 0.05$.

terized by enhanced migratory and invasive capacity of tumor cells. This is frequently associated with an enhanced mesenchymal- and stemness-like phenotype of tumor cells. In previous studies others and we demonstrated that the IGF2BP protein family is an essential modulator of cell migration during development and in cancer (44,49). In accord with these findings, others and we reported that IGF2BP1 enhances a mesenchymal-like cell phenotype in primary stem as well as tumor-derived cells (22,50). Accordingly, we hypothesized that inhibiting the expression of IGF2BP1 is essential for let-7 directed impairment of a mesenchymal-like cell phenotype with high migratory capacity.

In 2D-cultured ES-2 cells, the downregulation of let-7 activity by TuD-let-7 was associated with an enhanced formation of filopodia-like cell protrusions and a modestly reduced localization of ß-catenin (CTNNB1) at the cell periphery (Figure 8A; Supplementary Figure S8A). This was abolished by the depletion of IGF2BP1 and LIN28B leading to enhanced cell–cell contact formation and recruitment of CTNNB1 to the cell periphery. Notably, however, the depletion of LIN28B or IGF2BP1 failed to induce the formation of CDH1-containing adherens junctions (data not shown). In contrast to LIN28B and IGF2BP1, cell morphology and CTNNB1 localization remained essentially

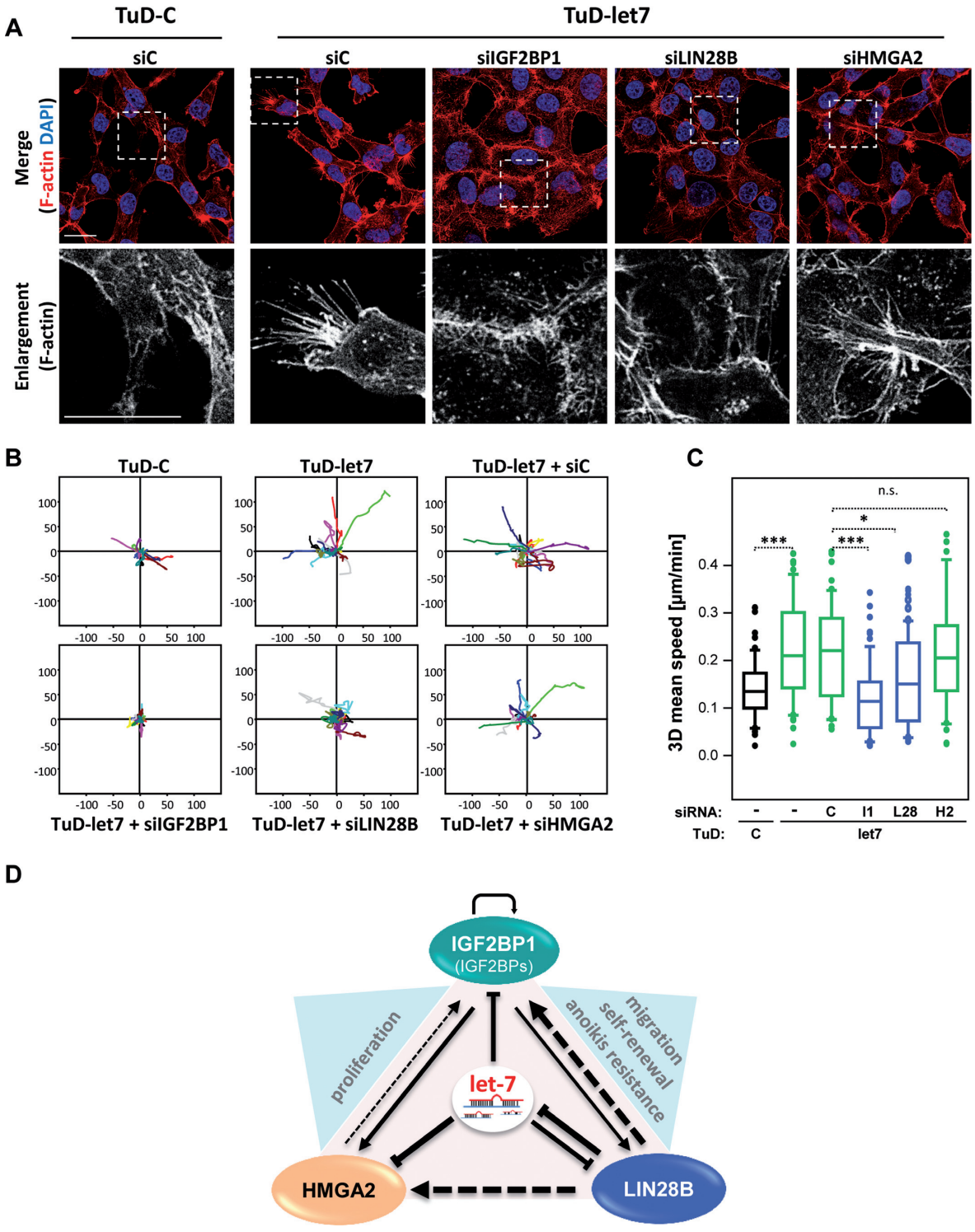

Figure 8. The LIN28B-IGF2BP1 axis antagonizes let-7 directed repression of 3D tumor cell migration. (**A**) The morphology of ES-2 cells transduced with decoys and transfected with siRNA pools as indicated was analyzed by F-actin labeling using Phalloidin-TRITC and staining of nuclei by DAPI. Representative images are shown. Enlargements of boxed regions (upper panel) are shown in the lower panel. Bars, 25 µm. (**B** and **C**) The migration of ES-2 cells transduced with decoys and transfected with siRNA pools as indicated was analyzed in 3D collagen matrices by time lapse live cell microscopy. The maximum projection of the 3D volumes was used to determine migratory paths (B) and speed of individual cells. The mean speed determined for individual cells (n > 100, analyzed cells) is depicted by box plots (C). Statistical significance was determined by a (two-sided) Student's *t*-test: $*P < 0.05$; $***P < 0.0005$; ns $P \geq 0.05$. (**D**) Schematic of the HMGA2-LIN28B-IGF2BP1 triangle with direct (solid lines) or indirect/non-characterized (dashed lines) regulation of expression. Line strength indicates the power of regulation (fold up-/downregulation). The let-7 miRNA family inhibits the expression of all three factors. IGF2BP1 enhances the expression of LIN28B, HMGA2 and itself by shielding mRNAs from let-7 attack. LIN28B controls the expression of HMGA2, IGF2BP1 and itself indirectly by repressing let-7 biogenesis. HMGA2 modestly enhances the expression of IGF2BP1, presumably by promoting IGF2BP1 mRNA synthesis. Prime let-7 antagonized tumor cell phenotypes enhanced by triangle factors are indicated in blue triangles.

unchanged by the knockdown of HMGA2 in ES-2 cells transduced with the let-7 decoy.

Supporting the observed enhancement of mesenchymal-like cell properties, the reduction of let-7 activity by TuD-let-7 resulted in increased 2D migration speed of ES-2 cells (Supplementary Figure S8B and C). Similar to effects on cell morphology, the depletion of LIN28B or IGF2BP1 but not HMGA2 abolished enhanced 2D migration observed in cells transduced with TuD-let-7. In contrast to modestly enhanced 2D migration, ES-2 cells stably transduced with the let-7 directed decoy showed a strongly elevated migratory capacity in 3D collagen matrices (Figure 8B and C). As observed for 2D migration, the migratory capacity of ES-2 cells in 3D matrices remained unaffected by the depletion of HMGA2 but was significantly reduced by the knockdown of LIN28B and almost completely abolished by siRNA-directed downregulation of IGF2BP1.

In conclusion these findings indicated that the let-7 family impairs mesenchymal-like tumor cell properties and 2D as well as 3D tumor cell migration. These tumor-suppressive roles are largely directed by the let-7 dependent inhibition of IGF2BP1 and LIN28B expression.

The IGF2BP-LIN28B-HMGA2 triangle is active in a broad range of cancers

Our findings suggest that IGF2BP1, LIN28B and HMGA2 antagonize let-7 action and thus promote an aggressive tumor cell phenotype. To determine if this positive feedback triangle could be active in a broad range of cancers, we searched for genes preferentially co-expressed with IGF2BP1 using the SEEK (51)) database. This revealed a striking positive correlation of IGF2BP1, LIN28B and HMGA2 expression in a variety of data sets (Supplementary Figure S9A). In contrast, no significant co-expression was observed for VCL serving as the negative control. This was further confirmed by microarray expression data of 917 tumor cell lines in the CCLE data set as well as by RNA-seq data of 45 OC-derived cell lines analyzed in the CCLE data set (Supplementary Figure S9B). These findings and the presented evidence for a let-7 antagonizing role of the triangle suggested a substantial co-expression of let-7 targeted mRNAs with IGF2BP1 and/or all triangle factors. To test this, a let-7 targeting score for the top 100 genes positively (red) or negatively (green) correlated with IGF2BP1 in the CCLE data set or all three triangle factors in SEEK (cancer data sets) was determined based on let-7 MRE predictions by the multi-MiR R package (52). This confirmed significantly higher top and median let-7 targeting scores for the co-expressed genes in both data sets (Supplementary Figure S9C). Intriguingly, IGF2BP2 and IGF2BP3 were among the positively associated genes in both data sets. In the triangle co-expression analyses in SEEK (cancer data sets) they even received the highest co-expression scores. This supported previous studies indicating IGF2BP3 to enhance HMGA2 expression (21). If all IGF2BP paralogues promote the expression of the other triangle factors was analyzed in ES-2 cells. The forced expression of all three GFP-tagged IGF2BPs resulted in upregulated expression of endogenous IGF2BP1 and HMGA2 (Supplementary Figure S9D). The abundance of LIN28B was only enhanced by IGF2BP1 and IGF2BP2 a finding requiring further investigation. Supporting previous studies, LIN28B expression substantially enhanced the expression of IGF2BP1, HMGA2 and itself whereas HMGA2 only modestly increased IGF2BP1 levels.

Finally, we analyzed the correlation of the triangle factors in a 2D gene view cross data set analysis via the R2 database. This revealed the most striking correlation across data sets as well as within samples for IGF2BP1 and LIN28B (Supplementary Figure S9E). Notably, a significant positive association was observed for three OC data sets (data not shown). A positive correlation across data sets was also observed for IGF2BP1 and HMGA2 as well as HMGA2 and LIN28B (Supplementary Figure S9F and G). However, in samples the correlation of IGF2BP1 or LIN28B with HMGA2 was weak or not significant, respectively (compare 'sample' in Supplementary Figure S9F and G versus Figure S9E).

In summary these findings provide strong evidence that the triangle consisting of IGF2BP1, LIN28B and HMGA2 (Figure 8D) is associated with the upregulation of let-7 target genes (including IGF2BP2 and IGF2BP3) and is active in a broad range of tumor-derived cells and primary cancers.

DISCUSSION

Our studies demonstrate that the tumor-suppressive role of the let-7 miRNA family is substantially antagonized by the self-promoting oncogenic 'triangle' composed of the architectural transcription factor HMGA2 and the RNA-binding proteins IGF2BP1 and LIN28B (Figure 8D). All 'triangle' factors are prime targets of the let-7 family previously identified in various independent studies, including gain-of-function analyses in distinct cancer-derived cells (4). In agreement, the levels of all three factors were substantially increased in OC-derived ES-2 cells transduced with let-7 directed tough decoys. This was associated with a significant enhancement of oncogenic tumor cell potential. The depletion of triangle factors in decoy-transduced ES-2 cells revealed that specific oncogenic properties were reduced in a factor-dependent manner (Figure 8D). Expression analyses showed that IGF2BP1 and LIN28B enhance the expression of all triangle factors whereas HMGA2 only modestly promoted the expression of IGF2BP1.

Although HMGA2 showed the most significant susceptibility to let-7 attack in loss- (here) and gain-of-function studies (4), it surprisingly had the weakest oncogenic potential of all triangle factors in ES-2 cells. In decoy transduced ES-2 cells the depletion of HMGA2 only impaired cell proliferation and spheroid growth when cells were cultured under permissive conditions, in the presence of FBS. This in agreement with previous observations indicating that the loss of HMGA2 for instance interferes with the growth of MEFs (53). The analysis of cell morphologies and 2D as well 3D cell migration analyses consistently showed that the depletion of HMGA2 in decoy-transduced cells remains ineffective. These findings relativize the view that HMGA2 enhances ovarian surface epithelial transformation by promoting epithelial-to-mesenchymal transition (EMT) (54). Various studies report that HMGA2 is a *bona fide* marker

of aggressive serous ovarian carcinoma (55) and proposed promising candidate for OC silencing therapy (56). However, in the Pamula-Pilat OC data set analyzed via the R2 database HMGA2 mRNA abundance was neither associated with event-free nor overall survival (data not shown). Moreover, HMGA2 showed the weakest association with the other triangle factors across cancer data sets (see Figure 8A–C) supporting its weak triangle promoting effects. Importantly, however, various studies report a pivotal tumor-suppressive role of the let-7 family in OC (48). Consistently, we observed that impairing let-7 activity substantially enhanced the oncogenic potential of OC-derived ES-2 cells. Hence, although the here presented *in vitro* analyses in OC-derived cells require further investigation by *in vivo* mouse models, our studies provide strong evidence that the let-7 directed inhibition of HMGA2 in cancer cells primarily modulates tumor growth under permissive conditions.

LIN28B was the most potent enhancer of triangle factor expression. When overexpressed (see Supplementary Figure S6D) it essentially abolished let-7 synthesis (data not shown) and stimulated the expression of IGF2BP1 (∼5-fold), itself (∼10-fold) and HMGA2 (∼12-fold). This enhancement of triangle factor expression was stronger than observed for impairing let-7 activity by decoys indicating the significant potency of LIN28B in suppressing let-7 biogenesis in cancer (10). Moreover, we cannot rule out that LIN28B also modulated the fate of triangle factor-encoding mRNAs directly and thus potentially independent of let-7 miRNAs. More importantly, however, LIN28B depletion in decoy-transduced ES-2 cells substantially impaired their self-renewal potential whereas it apparently was largely dispensable under permissive growth conditions (see Figure 7). Its pivotal role in determining self-renewal is largely consistent with findings in stem cells and other cancers (10,17). In ovarian epithelial cancer, recent studies reported that the expression of LIN28B and the IGF2BP1 homologue IGF2BP3 is associated with poor survival and confers platinum resistance in ovarian-cancer derived tumor cells (57). As shown here, LIN28B depletion significantly decreased the migration of decoy-transduced ES-2 cells and in agreement was reported to reduce cell migration when depleted in distinct OC-derived cells (57). In support of these findings, elevated expression of LIN28B was associated ($P = 0.02$) with reduced overall survival in the Pamula-Pilat data set (data not shown). Taken together these findings support the view that the inhibition of LIN28B by the let-7 family essentially impairs the self-renewal and stemness-like properties of OC cells.

The oncofetal protein IGF2BP1 was identified as a *bona fide* let-7 target in cancer-derived cells and suggested to escape let-7 directed regulation due to the shortening of its 3′ UTR by APA in aggressive cancers (4,18). In sharp contrast, we found that the expression of the longest IGF2BP1 transcripts is not reduced but rather increased in cancer-derived cells and most notably in aggressive OCs and neuroblastoma (see Figure 2; data not shown). This strongly suggests that the APA-dependent shortening of IGF2BP1's 3′ UTR is negligible in cancer. Instead our studies provide strong evidence that the enhanced expression of IGF2BP1 in aggressive cancers is largely due to the synergistic action of downregulated let-7 abundance and increased inhibition of let-7 directed regulation. Reduced let-7 levels are likely due to elevated LIN28A/B expression. In agreement, LIN28B and IGF2BP1 showed a strong positive correlation across cancer data sets and in cancer-derived cells, in which LIN28B was the most significantly and positively correlated factor according to expression data in the CCLE. Moreover, IGF2BP1 substantially enhanced the expression of all triangle factors, including itself, in a let-7 dependent manner. These findings are largely supported by previous studies showing that IGF2BP1 shields transcripts from let-7 independent miRNA attack, for instance miR-183 directed regulation of BTRC1 expression (19). Moreover, recent studies showed that IGF2BP3 protects HMGA2 transcripts from let-7 directed downregulation suggesting that all IGF2BPs antagonize miRNA-dependent regulation of their target mRNAs (21). In support of this, we observed that all IGF2BPs enhanced the expression of HMGA2 as well as IGF2BP1, and IGF2BP1/2 promoted the expression of LIN28B when overexpressed in ES-2 cells (see Supplementary Figure S9D). We propose that this 'safe-guard' role of IGF2BPs is largely facilitated via cytoplasmic mRNPs comprising IGF2BPs associated with 'virgin' mRNAs, which have not undergone the first round of mRNA translation, as previously suggested by others and us (41,42). In support of this, we isolated such mRNPs comprising IGF2BP1 associated with its target mRNA HMGA2, LIN28B and itself. Most notably, these mRNPs lack let-7 miRNAs and AGO proteins indicating that triangle factor-encoding transcripts are not subjected to let-7 directed regulation when associated with IGF2BP1 in virgin mRNPs. In ES-2 cells, the IGF2BP1-dependent association of target mRNAs with 'protective' mRNPs as well as triangle factor expression was increased with IGF2BP1 abundance. This indicates that the shielding of transcripts was associated with the enhanced expression of triangle factors. In summary, we propose that IGF2BP1 enhances the expression of triangle factors and potentially additional let-7 miRNA target mRNAs by shielding target transcripts from miRNA attack. This is further amplified by the LIN28B-dependent downregulation of let-7 levels. Thus, in concert, triangle factor enhance tumor cell aggressiveness via a self-promoting triangle until let-7 levels are diminished to negligible amounts, as for instance observed in HCC-derived Huh7 cells.

In OC, the association of elevated IGF2BP expression with poor patient prognosis supports this protective role (26–28). Moreover, our findings indicate that among all triangle factors analyzed in let-7 decoy-transduced ES-2 cells, IGF2BP1 depletion had the most severe effects. IGF2BP1 knockdown significantly reduced tumor cell proliferation and spheroid growth under permissive growth conditions confirming its largely cancer type-independent role in controlling tumor cell proliferation and tumor growth (26,58,59). More importantly, however, IGF2BP1 depletion essentially abolished the self-renewal potential of decoy-transduced ES-2 cells and thus showed an even higher oncogenic potential than LIN28B (see Figure 7D and E). Consistent with previous studies, IGF2BP1 depletion also impaired the 2D migration of decoy-transduced ES-2 cells and induced a MET-like (mesenchymal-epithelial-transition) morphological transition (22,44). Additionally, the first time analysis of IGF2BP1's role in 3D migra-

tion provide strong evidence that IGF2BP1 enhances the dissemination of OC cells also *in vivo*, as previously observed in a breast cancer mouse model (60). Notably, pro-migratory and growth promoting roles were assigned to all three IGF2BPs in OC-derived cells providing further evidence that all three IGF2BPs enhance the oncogenic potential of the let-7 antagonizing triangle (28,57).

In conclusion our findings indicate that the tumor-suppressive roles of the let-7 family are antagonized by a potent and self-promoting triangle consisting of IGF2BP1 (potentially all IGF2BPs), LIN28B and HMGA2. Although *in vivo* analyses and studies in other cancers are required, we provide evidence that the identified let-7 antagonizing triangle is probably active in a broad range of cancers, a finding supported by previous studies in neuroblastoma and liver cancer (11,12). Future studies now have to aim at impairing the potency of this triangle. From our point of view the most promising strategy is the concomitant impairment of LIN28B's role in suppressing let-7 biogenesis and the downregulation of IGF2BP1 expression. This would enhance the abundance of the tumor-suppressive let-7 miRNA family and simultaneously would decrease let-7 directed shielding activity by IGF2BP1.

SUPPLEMENTARY DATA

Supplementary Data are available at NAR Online.

ACKNOWLEDGEMENT

The authors thank Knut Krohn at the Core Unit DNA Technologies IZKF, University of Leipzig for RNA Sequencing. The authors gratefully thank Gunther Meister, University of Regensburg; Christiane Rammelt, University of Halle and Christine Mayr, Memorial Sloan Kettering Cancer Center, New York for technical support and reagents.

Author contribution: B.B., N.B. and S.H. designed the experiments. B.B., N.B. and S.M. carried out and interpreted the experiments. M.L. generated constructs and stable cell populations (overexpression and CRISPR/Cas). M.G. and D.M analyzed RNA sequencing data. M.V and C.T provided tumor samples. M.V. and N.B. carried out the patient sample analyses. S.H. conceived the experimental design and wrote the manuscript.

FUNDING

Deutsche Forschungsgemeinschaft (DFG) [GRK1591 to S.H.]. Funding for open access charge: DFG Funding [GRK1591 to S.H.].

Conflict of interest statement. None declared.

REFERENCES

1. Jonas,S. and Izaurralde,E. (2015) Towards a molecular understanding of microRNA-mediated gene silencing. *Nat. Rev. Genet.*, **16**, 421–433.
2. Reinhart,B.J., Slack,F.J., Basson,M., Pasquinelli,A.E., Bettinger,J.C., Rougvie,A.E., Horvitz,H.R. and Ruvkun,G. (2000) The 21-nucleotide let-7 RNA regulates developmental timing in Caenorhabditis elegans. *Nature*, **403**, 901–906.
3. Roush,S. and Slack,F.J. (2008) The let-7 family of microRNAs. *Trends Cell Biol.*, **18**, 505–516.
4. Boyerinas,B., Park,S.M., Shomron,N., Hedegaard,M.M., Vinther,J., Andersen,J.S., Feig,C., Xu,J., Burge,C.B. and Peter,M.E. (2008) Identification of let-7-regulated oncofetal genes. *Cancer Res.*, **68**, 2587–2591.
5. Young,A.R. and Narita,M. (2007) Oncogenic HMGA2: short or small? *Genes Dev.*, **21**, 1005–1009.
6. Mayr,C., Hemann,M.T. and Bartel,D.P. (2007) Disrupting the pairing between let-7 and Hmga2 enhances oncogenic transformation. *Science*, **315**, 1576–1579.
7. Lee,Y.S. and Dutta,A. (2007) The tumor suppressor microRNA let-7 represses the HMGA2 oncogene. *Genes Dev.*, **21**, 1025–1030.
8. Viswanathan,S.R., Daley,G.Q. and Gregory,R.I. (2008) Selective blockade of microRNA processing by Lin28. *Science*, **320**, 97–100.
9. Piskounova,E., Polytarchou,C., Thornton,J.E., LaPierre,R.J., Pothoulakis,C., Hagan,J.P., Iliopoulos,D. and Gregory,R.I. (2011) Lin28A and Lin28B inhibit let-7 microRNA biogenesis by distinct mechanisms. *Cell*, **147**, 1066–1079.
10. Wang,T., Wang,G., Hao,D., Liu,X., Wang,D., Ning,N. and Li,X. (2015) Aberrant regulation of the LIN28A/LIN28B and let-7 loop in human malignant tumors and its effects on the hallmarks of cancer. *Mol. Cancer*, **14**, 125.
11. Nguyen,L.H., Robinton,D.A., Seligson,M.T., Wu,L., Li,L., Rakheja,D., Comerford,S.A., Ramezani,S., Sun,X., Parikh,M.S. *et al.* (2014) Lin28b is sufficient to drive liver cancer and necessary for its maintenance in murine models. *Cancer Cell*, **26**, 248–261.
12. Molenaar,J.J., Domingo-Fernandez,R., Ebus,M.E., Lindner,S., Koster,J., Drabek,K., Mestdagh,P., van Sluis,P., Valentijn,L.J., van Nes,J. *et al.* (2012) LIN28B induces neuroblastoma and enhances MYCN levels via let-7 suppression. *Nat. Genet.*, **44**, 1199–1206.
13. Lederer,M., Bley,N., Schleifer,C. and Huttelmaier,S. (2014) The role of the oncofetal IGF2 mRNA-binding protein 3 (IGF2BP3) in cancer. *Semin. Cancer Biol.*, **29C**, 3–12.
14. Bell,J.L., Wachter,K., Muhleck,B., Pazaitis,N., Kohn,M., Lederer,M. and Huttelmaier,S. (2013) Insulin-like growth factor 2 mRNA-binding proteins (IGF2BPs): post-transcriptional drivers of cancer progression? *Cell. Mol. Life Sci.*, **70**, 2657–2675.
15. Hammer,N.A., Hansen,T., Byskov,A.G., Rajpert-De Meyts,E., Grondahl,M.L., Bredkjaer,H.E., Wewer,U.M., Christiansen,J. and Nielsen,F.C. (2005) Expression of IGF-II mRNA-binding proteins (IMPs) in gonads and testicular cancer. *Reproduction*, **130**, 203–212.
16. Christiansen,J., Kolte,A.M., Hansen,T. and Nielsen,F.C. (2009) IGF2 mRNA-binding protein 2: biological function and putative role in type 2 diabetes. *J. Mol. Endocrinol.*, **43**, 187–195.
17. Shyh-Chang,N. and Daley,G.Q. (2013) Lin28: primal regulator of growth and metabolism in stem cells. *Cell Stem Cell*, **12**, 395–406.
18. Mayr,C. and Bartel,D.P. (2009) Widespread shortening of 3′ UTRs by alternative cleavage and polyadenylation activates oncogenes in cancer cells. *Cell*, **138**, 673–684.
19. Elcheva,I., Goswami,S., Noubissi,F.K. and Spiegelman,V.S. (2009) CRD-BP protects the coding region of betaTrCP1 mRNA from miR-183-mediated degradation. *Mol. Cell*, **35**, 240–246.
20. Goswami,S., Tarapore,R.S., Teslaa,J.J., Grinblat,Y., Setaluri,V. and Spiegelman,V.S. (2010) MicroRNA-340-mediated degradation of microphthalmia-associated transcription factor mRNA is inhibited by the coding region determinant-binding protein. *J. Biol. Chem.*, **285**, 20532–20540.
21. Jonson,L., Christiansen,J., Hansen,T.V., Vikesa,J., Yamamoto,Y. and Nielsen,F.C. (2014) IMP3 RNP safe houses prevent miRNA-directed HMGA2 mRNA decay in cancer and development. *Cell Rep.*, **7**, 539–551.
22. Zirkel,A., Lederer,M., Stohr,N., Pazaitis,N. and Huttelmaier,S. (2013) IGF2BP1 promotes mesenchymal cell properties and migration of tumor-derived cells by enhancing the expression of LEF1 and SNAI2 (SLUG). *Nucleic Acids Res.*, **41**, 6618–6636.
23. Noubissi,F.K., Elcheva,I., Bhatia,N., Shakoori,A., Ougolkov,A., Liu,J., Minamoto,T., Ross,J., Fuchs,S.Y. and Spiegelman,V.S. (2006) CRD-BP mediates stabilization of betaTrCP1 and c-myc mRNA in response to beta-catenin signalling. *Nature*, **441**, 898–901.
24. Barretina,J., Caponigro,G., Stransky,N., Venkatesan,K., Margolin,A.A., Kim,S., Wilson,C.J., Lehar,J., Kryukov,G.V., Sonkin,D. *et al.* (2012) The cancer cell line encyclopedia enables predictive modelling of anticancer drug sensitivity. *Nature*, **483**, 603–607.

25. Nielsen,J., Christiansen,J., Lykke-Andersen,J., Johnsen,A.H., Wewer,U.M. and Nielsen,F.C. (1999) A family of insulin-like growth factor II mRNA-binding proteins represses translation in late development. *Mol. Cell. Biol.*, **19**, 1262–1270.
26. Kobel,M., Weidensdorfer,D., Reinke,C., Lederer,M., Schmitt,W.D., Zeng,K., Thomssen,C., Hauptmann,S. and Huttelmaier,S. (2007) Expression of the RNA-binding protein IMP1 correlates with poor prognosis in ovarian carcinoma. *Oncogene*, **26**, 7584–7589.
27. Kobel,M., Xu,H., Bourne,P.A., Spaulding,B.O., Shih Ie,M., Mao,T.L., Soslow,R.A., Ewanowich,C.A., Kalloger,S.E., Mehl,E. *et al.* (2009) IGF2BP3 (IMP3) expression is a marker of unfavorable prognosis in ovarian carcinoma of clear cell subtype. *Mod. Pathol.*, **22**, 469–475.
28. Davidson,B., Rosenfeld,Y.B., Holth,A., Hellesylt,E., Trope,C.G., Reich,R. and Yisraeli,J.K. (2014) VICKZ2 protein expression in ovarian serous carcinoma effusions is associated with poor survival. *Hum. Pathol.*, **45**, 1520–1528.
29. Anglesio,M.S., Arnold,J.M., George,J., Tinker,A.V., Tothill,R., Waddell,N., Simms,L., Locandro,B., Fereday,S., Traficante,N. *et al.* (2008) Mutation of ERBB2 provides a novel alternative mechanism for the ubiquitous activation of RAS-MAPK in ovarian serous low malignant potential tumors. *Mol. Cancer Res.*, **6**, 1678–1690.
30. Tothill,R.W., Tinker,A.V., George,J., Brown,R., Fox,S.B., Lade,S., Johnson,D.S., Trivett,M.K., Etemadmoghadam,D., Locandro,B. *et al.* (2008) Novel molecular subtypes of serous and endometrioid ovarian cancer linked to clinical outcome. *Clin. Cancer Res.*, **14**, 5198–5208.
31. Glasmacher,E., Hoefig,K.P., Vogel,K.U., Rath,N., Du,L., Wolf,C., Kremmer,E., Wang,X. and Heissmeyer,V. (2010) Roquin binds inducible costimulator mRNA and effectors of mRNA decay to induce microRNA-independent post-transcriptional repression. *Nat. Immunol.*, **11**, 725–733.
32. Gurtan,A.M., Ravi,A., Rahl,P.B., Bosson,A.D., JnBaptiste,C.K., Bhutkar,A., Whittaker,C.A., Young,R.A. and Sharp,P.A. (2013) Let-7 represses Nr6a1 and a mid-gestation developmental program in adult fibroblasts. *Genes Dev.*, **27**, 941–954.
33. Rebucci,M., Sermeus,A., Leonard,E., Delaive,E., Dieu,M., Fransolet,M., Arnould,T. and Michiels,C. (2015) miRNA-196b inhibits cell proliferation and induces apoptosis in HepG2 cells by targeting IGF2BP1. *Mol. Cancer*, **14**, 79.
34. Braun,J., Misiak,D., Busch,B., Krohn,K. and Huttelmaier,S. (2014) Rapid identification of regulatory microRNAs by miTRAP (miRNA trapping by RNA in vitro affinity purification). *Nucleic Acids Res.*, **42**, e66.
35. Sideris,M. and Papagrigoriadis,S. (2014) Molecular biomarkers and classification models in the evaluation of the prognosis of colorectal cancer. *Anticancer Res.*, **34**, 2061–2068.
36. Ohdaira,H., Sekiguchi,M., Miyata,K. and Yoshida,K. (2012) MicroRNA-494 suppresses cell proliferation and induces senescence in A549 lung cancer cells. *Cell Prolif.*, **45**, 32–38.
37. Wang,R.J., Li,J.W., Bao,B.H., Wu,H.C., Du,Z.H., Su,J.L., Zhang,M.H. and Liang,H.Q. (2015) MicroRNA-873 (miRNA-873) inhibits glioblastoma tumorigenesis and metastasis by suppressing the expression of IGF2BP1. *J. Biol. Chem.*, **290**, 8938–8948.
38. Huang,X., Huang,M., Kong,L. and Li,Y. (2015) miR-372 suppresses tumour proliferation and invasion by targeting IGF2BP1 in renal cell carcinoma. *Cell Prolif.*, **48**, 593–599.
39. Alajez,N.M., Shi,W., Wong,D., Lenarduzzi,M., Waldron,J., Weinreb,I. and Liu,F.F. (2012) Lin28b promotes head and neck cancer progression via modulation of the insulin-like growth factor survival pathway. *Oncotarget*, **3**, 1641–1652.
40. Domcke,S., Sinha,R., Levine,D.A., Sander,C. and Schultz,N. (2013) Evaluating cell lines as tumour models by comparison of genomic profiles. *Nat. Commun.*, **4**, 2126.
41. Jonson,L., Vikesaa,J., Krogh,A., Nielsen,L.K., Hansen,T., Borup,R., Johnsen,A.H., Christiansen,J. and Nielsen,F.C. (2007) Molecular composition of IMP1 ribonucleoprotein granules. *Mol. Cell. Proteomics*, **6**, 798–811.
42. Weidensdorfer,D., Stohr,N., Baude,A., Lederer,M., Kohn,M., Schierhorn,A., Buchmeier,S., Wahle,E. and Huttelmaier,S. (2009) Control of c-myc mRNA stability by IGF2BP1-associated cytoplasmic RNPs. *RNA*, **15**, 104–115.
43. Huttelmaier,S., Zenklusen,D., Lederer,M., Dictenberg,J., Lorenz,M., Meng,X., Bassell,G.J., Condeelis,J. and Singer,R.H. (2005) Spatial regulation of beta-actin translation by Src-dependent phosphorylation of ZBP1. *Nature*, **438**, 512–515.
44. Stohr,N., Kohn,M., Lederer,M., Glass,M., Reinke,C., Singer,R.H. and Huttelmaier,S. (2012) IGF2BP1 promotes cell migration by regulating MK5 and PTEN signaling. *Genes Dev.*, **26**, 176–189.
45. Hafner,M., Landthaler,M., Burger,L., Khorshid,M., Hausser,J., Berninger,P., Rothballer,A., Ascano,M. Jr, Jungkamp,A.C., Munschauer,M. *et al.* (2010) Transcriptome-wide identification of RNA-binding protein and microRNA target sites by PAR-CLIP. *Cell*, **141**, 129–141.
46. Wachter,K., Kohn,M., Stohr,N. and Huttelmaier,S. (2013) Subcellular localization and RNP formation of IGF2BPs (IGF2 mRNA-binding proteins) is modulated by distinct RNA-binding domains. *Biol. Chem.*, **394**, 1077–1090.
47. Brants,J.R., Ayoubi,T.A., Chada,K., Marchal,K., Van de Ven,W.J. and Petit,M.M. (2004) Differential regulation of the insulin-like growth factor II mRNA-binding protein genes by architectural transcription factor HMGA2. *FEBS Lett.*, **569**, 277–283.
48. van Jaarsveld,M.T., Helleman,J., Berns,E.M. and Wiemer,E.A. (2010) MicroRNAs in ovarian cancer biology and therapy resistance. *Int. J. Biochem. Cell Biol.*, **42**, 1282–1290.
49. Yaniv,K., Fainsod,A., Kalcheim,C. and Yisraeli,J.K. (2003) The RNA-binding protein Vg1 RBP is required for cell migration during early neural development. *Development*, **130**, 5649–5661.
50. Mahaira,L.G., Katsara,O., Pappou,E., Iliopoulou,E.G., Fortis,S., Antsaklis,A., Fotinopoulos,P., Baxevanis,C.N., Papamichail,M. and Perez,S.A. (2014) IGF2BP1 expression in human mesenchymal stem cells significantly affects their proliferation and is under the epigenetic control of TET1/2 demethylases. *Stem Cells Dev.*, **23**, 2501–2512.
51. Zhu,Q., Wong,A.K., Krishnan,A., Aure,M.R., Tadych,A., Zhang,R., Corney,D.C., Greene,C.S., Bongo,L.A., Kristensen,V.N. *et al.* (2015) Targeted exploration and analysis of large cross-platform human transcriptomic compendia. *Nat. Methods*, **12**, 211–214.
52. Ru,Y., Kechris,K.J., Tabakoff,B., Hoffman,P., Radcliffe,R.A., Bowler,R., Mahaffey,S., Rossi,S., Calin,G.A., Bemis,L. *et al.* (2014) The multiMiR R package and database: integration of microRNA-target interactions along with their disease and drug associations. *Nucleic Acids Res.*, **42**, e133.
53. Zhou,X., Benson,K.F., Ashar,H.R. and Chada,K. (1995) Mutation responsible for the mouse pygmy phenotype in the developmentally regulated factor HMGI-C. *Nature*, **376**, 771–774.
54. Wu,J., Liu,Z., Shao,C., Gong,Y., Hernando,E., Lee,P., Narita,M., Muller,W., Liu,J. and Wei,J.J. (2011) HMGA2 overexpression-induced ovarian surface epithelial transformation is mediated through regulation of EMT genes. *Cancer Res.*, **71**, 349–359.
55. Mahajan,A., Liu,Z., Gellert,L., Zou,X., Yang,G., Lee,P., Yang,X. and Wei,J.J. (2010) HMGA2: a biomarker significantly overexpressed in high-grade ovarian serous carcinoma. *Modern Pathol.*, **23**, 673–681.
56. Malek,A., Bakhidze,E., Noske,A., Sers,C., Aigner,A., Schafer,R. and Tchernitsa,O. (2008) HMGA2 gene is a promising target for ovarian cancer silencing therapy. *Int. J. Cancer*, **123**, 348–356.
57. Hsu,K.F., Shen,M.R., Huang,Y.F., Cheng,Y.M., Lin,S.H., Chow,N.H., Cheng,S.W., Chou,C.Y. and Ho,C.L. (2015) Overexpression of the RNA-binding proteins Lin28B and IGF2BP3 (IMP3) is associated with chemoresistance and poor disease outcome in ovarian cancer. *Br. J. Cancer*, **113**, 414–424.
58. Gutschner,T., Hammerle,M., Pazaitis,N., Bley,N., Fiskin,E., Uckelmann,H., Heim,A., Grobeta,M., Hofmann,N., Geffers,R. *et al.* (2014) Insulin-like growth factor 2 mRNA-binding protein 1 (IGF2BP1) is an important protumorigenic factor in hepatocellular carcinoma. *Hepatology*, **59**, 1900–1911.
59. Bell,J.L., Turlapati,R., Liu,T., Schulte,J.H. and Huttelmaier,S. (2015) IGF2BP1 harbors prognostic significance by gene gain and diverse expression in neuroblastoma. *J. Clin. Oncol.*, **33**, 1285–1293.
60. Tessier,C.R., Doyle,G.A., Clark,B.A., Pitot,H.C. and Ross,J. (2004) Mammary tumor induction in transgenic mice expressing an RNA-binding protein. *Cancer Res.*, **64**, 209–214.
61. Haraguchi,T., Ozaki,Y. and Iba,H. (2009) Vectors expressing efficient RNA decoys achieve the long-term suppression of specific microRNA activity in mammalian cells. *Nucleic Acids Res.*, **37**, e43.
62. Sambrook,J. and Russell,D.W. (2006) Separation of RNA According to Size: Electrophoresis of Glyoxylated RNA through Agarose Gels. *CSH Protoc.*, **2006**, doi:10.1101/pdb.prot4057.

63. Kohn,M., Pazaitis,N. and Huttelmaier,S. (2013) Why YRNAs? About Versatile RNAs and Their Functions. *Biomolecules*, **3**, 143–156.
64. Lisowska,K.M., Olbryt,M., Dudaladava,V., Pamula-Pilat,J., Kujawa,K., Grzybowska,E., Jarzab,M., Student,S., Rzepecka,I.K., Jarzab,B. *et al.* (2014) Gene expression analysis in ovarian cancer - faults and hints from DNA microarray study. *Front. Oncol.*, **4**, 6.
65. Molenaar,J.J., Koster,J., Zwijnenburg,D.A., van Sluis,P., Valentijn,L.J., van der Ploeg,I., Hamdi,M., van Nes,J., Westerman,B.A., van Arkel,J. *et al.* (2012) Sequencing of neuroblastoma identifies chromothripsis and defects in neuritogenesis genes. *Nature*, **483**, 589–593.
66. Ran,F.A., Hsu,P.D., Wright,J., Agarwala,V., Scott,D.A. and Zhang,F. (2013) Genome engineering using the CRISPR-Cas9 system. *Nat. Protoc.*, **8**, 2281–2308.
67. Hannus,M., Beitzinger,M., Engelmann,J.C., Weickert,M.T., Spang,R., Hannus,S. and Meister,G. (2014) siPools: highly complex but accurately defined siRNA pools eliminate off-target effects. *Nucleic Acids Res.*, **42**, 8049–8061.
68. Stohr,N., Lederer,M., Reinke,C., Meyer,S., Hatzfeld,M., Singer,R.H. and Huttelmaier,S. (2006) ZBP1 regulates mRNA stability during cellular stress. *J. Cell Biol.*, **175**, 527–534.